**Dissertationes Forestales 238**

# Dynamics and biophysical controls of carbon, water and energy exchange over a semiarid shrubland in northern China

Xin Jia

School of Forest Sciences
Faculty of Science and Forestry
University of Eastern Finland

Academic dissertation

To be presented, with the permission of the Faculty of Science and Forestry of the University of Eastern Finland, for public examination in auditorium BOR 100 in borealis building on Joensuu campus of the University of Eastern Finland, Yliopistokatu 7, Joensuu on 23 May 2017 at 12 o' clock noon.

*Title of dissertation:* Dynamics and biophysical controls of carbon, water and energy exchange over a semiarid shrubland in northern China

*Author:* Xin Jia

*Dissertationes Forestales 238*

https://doi.org/10.14214/df.238


*Thesis Supervisors:*
Professor Heli Peltola
School of Forest Sciences, University of Eastern Finland, Joensuu, Finland
Professor Tianshan Zha
School of Soil and Water Conservation, Beijing Forestry University, Beijing, China
Dr. Jinnan Gong (co-supervisor)
School of Forest Sciences, University of Eastern Finland, Joensuu, Finland

*Pre-examiners:*
Docent Samuli Launiainen
Natural Resources Institute Finland, Helsinki, Finland
Professor Bjarni D. Sigurdsson
Faculty of Natural Resources and Environmental Sciences, Agricultural University of Iceland, Borgarnes, Iceland

*Opponent:*
Professor Timo Vesala
Department of Physics, University of Helsinki, Helsinki, Finland

ISSN 1795-7389 (online)
ISBN 978-951-651-566-6 (pdf)

ISSN 2323-9220 (pint)
ISBN 978-951-651-567-3 (paperback)

*Publishers:*
Finnish Society of Forest Science
Faculty of Agriculture and Forestry at the University of Helsinki
School of Forest Sciences at the University of Eastern Finland

*Editorial Office:*
Finnish Society of Forest Science
Viikinkaari 6, FI-00790 Helsinki, Finland
http://www.dissertationesforestales.fi

**Jia X.** (2017). Dynamics and biophysical controls of carbon, water and energy exchange over a semiarid shrubland in northern China. Dissertationes Forestales 238. 36p. Available at: https://doi.org/10.14214/df.238

## ABSTRACT

The main aim of this study was to investigate the dynamics and biophysical controls of carbon, water and energy exchange over a semiarid shrub ecosystem in the Mu Us desert, northern China, using continuous eddy-covariance (EC) measurements. Specific objectives were as follows: (1) To examine intra-annual variations in net ecosystem $CO_2$ exchange (*NEE)* and its biophysical controls (Paper I); (2) To quantify the diurnal and seasonal variations in surface energy-balance components, and to examine the partitioning of net radiation ($R_n$) among different energy components at diurnal and seasonal timescales (Paper II); and (3) To examine how ecosystem production and water use efficiency (*WUE)* vary inter-annually with contrasting precipitation (*PPT*) and soil moisture patterns (Paper III).

The results showed that, soil water content (i.e. at 30 cm depth, *SWC*_30), or water deficit, imposed a major control on the seasonal dynamics of carbon assimilation and energy partitioning. Water deficit (i.e. *SWC*_30 < 0.10 $m^3$ $m^{-3}$) was a major constraint over daytime *NEE*, and also interacted with other stresses, e.g. heat stress and photoinhibition (Paper I). Low soil moisture reduced the temperature sensitivity ($Q_{10}$) of total ecosystem respiration (*TER*). Rain events triggered immediate pulses of carbon release from the ecosystem, followed by peaks of $CO_2$ uptake 1–2 days later. Leaf area index (*LAI*) accounted for 45 and 65% of the seasonal variation in *NEE* and gross ecosystem production (*GEP*), respectively. On the other hand, sensible heat flux (*H*) exceeded latent heat flux ($\lambda E$) during most time of the year (Paper II). The evaporative fraction (*EF*, i.e. $\lambda E/R_n$), Priestley-Taylor coefficient ($\alpha$), surface conductance ($g_s$) and decoupling coefficient ($\Omega$) all correlated positively with *SWC*_30 and *LAI*. The direct enhancement of $\lambda E$ by high vapor pressure deficit (*VPD*) was buffered by a concurrent suppression of $g_s$, which controlled *EF* and $\alpha$ by mediating the effects of *LAI*, *SWC*_30 and *VPD*.

At the annual scale, net ecosystem production (*NEP*, here defined as −*NEE*) indicated a rapid shift from an annual sink of carbon in 2012 (*NEP* = 77 ± 10 g C $m^{-2}$ $yr^{-1}$) to a source of carbon in 2014 (*NEP* = -22 ± 5 g C $m^{-2}$ $yr^{-1}$), with the year 2013 being close to carbon neutral (*NEP* = -4 ± 10 g C $m^{-2}$ $yr^{-1}$) (Paper III). *GEP*, *TER* and evapotranspiration (*ET*) also declined over the three years. Suppressed annual carbon and water fluxes were observed in years with low spring soil moisture. *GEP* declined more than *TER* and *ET*, leading to reduced carbon sequestration and *WUE* (i.e. *GEP*/*ET*). Neither annual nor growing-season *PPT* amount could explain the year-to-year variation in carbon fluxes. *ET* was a better proxy for water available to ecosystem carbon exchange on an annual basis. Autumn soil moisture levels were carried over winter to spring, and affected the rates of leafout, plant growth and carbon uptake in the early- to mid-growing season.

**Keywords:** Carbon balance, eddy-covariance, evapotranspiration, energy balance, shrubland, water availability

## ACKNOWLEDGEMENTS

This study was carried out under the Finnish-Chinese research collaboration project EXTREME, between Beijing Forestry University (BFU), School of Soil and Water Conservation (team led by Prof. Tianshan Zha) and University of Eastern Finland (UEF), School of Forest Sciences (team led by Prof. Heli Peltola). The project was funded jointly by the National Natural Science Foundation of China (NSFC, Proj. No. 31361130340), the Academy of Finland and UEF (Proj. No. 14921) for years 2013–2016. All instruments used in this work were funded by BFU. This work was also financially supported by the Fundamental Research Funds for the Central Universities (Proj. No. 2015ZCQ-SB-02). I gratefully acknowledge all funding sources that supported this work.

I wish to express my sincere gratitude to my supervisors, Prof. Heli Peltola, Prof. Tianshan Zha and Dr. Jinnan Gong, for their guidance and support throughout the research work. Special thanks are extended to the U.S.–China Carbon Consortium (USCCC) for supporting this work via helpful discussions and the exchange of ideas, and to the Bureau of Environmental Projection and Forestry at Yanchi County, Ningxia, China for providing logistical support. I am grateful to Dr. Alan Barr for providing valuable help in data analysis, paper writing and language editing. I am also grateful to the two pre-examiners, Docent Samuli Launiainen and Prof. Bjarni D. Sigurdsson, for their evaluation and comments on this dissertation. I would like to thank Xuewu Yang, Shijun Liu, Guopeng Chen, Ben Wang, Peng Liu, Jiawei Mu for assistance with field measurements and instrument maintenance. My colleagues, including Prof. Bin Wu, Prof. Yuqing Zhang, Dr. Shugao Qin, Dr. Wei Feng and Dr. Zongrui Lai and others, also supported my research work in many ways.

Finally, I would like to dedicate this thesis to my wife, Dr. Xiaodong Zhang, who supported my research work in all possible ways. I am especially grateful to my parents (Shaoyu Jia and Qin Xiao) for their persistent support. Last but not least, I would like to thank all my friends in Joensuu, Beijing and Yanchi for the wonderful days we spent together.

In Beijing, April 2017

Xin Jia

## LIST OF ORIGINAL ARTICLES

This thesis is based on the following three articles, which will be referred to by Roman numbers I–III in the text. The three articles are reprinted with the kind permission of the publishers or with the rights retained as author.

I. Jia X., Zha T.S., Wu B., Zhang Y.Q., Gong J.N., Qin S.G., Chen G.P., Kellomäki S., Peltola H. (2014). Biophysical controls on net ecosystem $CO_2$ exchange over a semiarid shrubland in northwest China. Biogeosciences 11: 4679–4693
http://dx.doi.org/10.5194/bg-11-4679-2014

II. Jia X., Zha T.S., Gong J.N., Wu B., Zhang Y.Q., Qin S.G., Chen G.P., Feng W., Kellomäki S., Peltola H. (2016). Energy partitioning over a semi-arid shrubland in northern China. Hydrological Processes 30: 972–985
http://dx.doi.org/10.1002/hyp.10685

III. Jia X., Zha T., Gong J., Wang B., Zhang Y., Wu B., Qin S., Peltola H. (2016). Carbon and water exchange over a temperate semi-arid shrubland during three years of contrasting precipitation and soil moisture patterns. Agricultural and Forest Meteorology 228: 120–129
http://dx.doi.org/10.1016/j.agrformet.2016.07.007

The present author, Xin Jia, was mainly responsible for data processing, analysis and manuscript writing for Articles I–III. The co-authors contributed to the articles via work related to the implementation of research tasks, field measurements and manuscript revisions.

## TABLE OF CONTENTS

# LIST OF SYMBOLS AND ABBREVIATIONS

*EF*, Evaporative fraction
*ET*, Evapotranspiration
$g_s$, Bulk surface conductance
*G*, Soil heat flux
*GEP*, Gross ecosystem production
*H*, Sensible heat flux
*LAI*, Leaf area index
*NEE*, Net ecosystem $CO_2$ exchange
$NEE_{day}$, Daytime net ecosystem $CO_2$ exchange
$NEE_{max}$, Maximum rate of net $CO_2$ uptake
$NEE_{night}$, Nighttime net ecosystem $CO_2$ exchange
*NEP*, Net ecosystem production
*NPP*, Net primary production
*PAR*, Photosynthetically active radiation
*PPT*, Precipitation
$Q_{10}$, Temperature sensitivity of ecosystem respiration
$R_d$, Average daytime ecosystem respiration
$R_{e10}$, Ecosystem respiration at a reference $T_s$ of 10 ℃
*REW*, relative extractable water
$R_n$, Net radiation
*SWC*, Soil water content
$T_a$, Air temperature
$T_s$, Soil temperature
*TER*, Total ecosystem respiration
$u^*$, Friction velocity
*VPD*, Vapor pressure deficit
*WUE*, water use efficiency
$\alpha$, Priestley-Taylor coefficient
$\beta$, Bowen ratio
$\lambda E$, Latent heat flux
$\lambda E_{eq}$, Equilibrium $\lambda E$
$\Omega$, Decoupling coefficient

# 1. INTRODUCTION

## 1.1 Dryland ecosystems and climate change

Drylands (semiarid and arid areas) comprise over 40% of the global terrestrial surface and are home to more than 38% of the global population (Reynolds et al. 2007; Gao et al. 2012). The extent of dryland ecosystems has been expanding in many regions around the world due to climate change and increasing human activities (Asner et al. 2003). Climatic change driven by atmospheric $CO_2$ enrichment could lead to a global increase in desert areas by 17% (Emanuel et al., 1985). Arid and semiarid areas in China span from central Asia in the west to northern China in the east, covering an area of more than 1.6 million $km^2$ (Wang et al. 2008). These areas lie primarily in regions above 35° N and have an annual rainfall of <450 mm. In China, the total desertified area increased by 2460 $km^2$ $yr^{-1}$ from the 1980s to the mid-1990s (Yang et al. 2005).

Although dryland ecosystems are characterized by low precipitation (*PPT*), soil fertility, aboveground biomass and productivity, they constitute an important component of the global carbon cycle (Poulter et al. 2014; Ahlström et al. 2015). Arid and semiarid areas account for approximately 20–35% of total terrestrial net primary productivity (*NPP*) (Field et al. 1998) and 15–20% of total soil organic carbon (Lal 2004; Liu et al. 2016). Some dryland ecosystems have shown a significant carbon sequestration potential, both through photosynthesis by plants (shrubs and grasses) (Gao et al. 2012) and $CO_2$ absorption by alkaline soils (Wohlfahrt et al. 2008; Xie et al. 2009). Recent evidence suggests an increasingly important role of semiarid ecosystems in driving the trend and interannual variability of the global carbon cycle (Poulter et al. 2014; Ahlström et al. 2015). Despite the importance of drylands, carbon, water and energy exchanges and their influencing factors are less well understood in these ecosystems compared to mesic forests and grasslands (Scott et al. 2015; Biederman et al. 2016; Liu et al. 2016), limiting our ability to project the global carbon balance under changing climate. In particular, the arid and semiarid shrublands of northern China, which represent an important land-cover type in Eurasia, are subject to increasing temperatures and altered *PPT* patterns (Liu et al. 2011; Gao et al. 2012). However, arid and semiarid ecosystems dominated by shrub species are largely under-represented in studies of climate change impacts (Liu et al. 2016).

Dryland ecosystems are highly sensitive to changes in climate (e.g. rising temperatures and shifting *PPT* patterns) (Li et al. 2005; Liu et al. 2016; Zhang et al. 2016), and their responses to climatic variability may feed back to the regional or global climate system (Poulter et al. 2014; Ahlström et al. 2015). Global climate models suggest a warmer and drier future climate in semiarid and arid regions of Asia (McCarthy et al. 2001). China's average temperature had increased by 1.2 °C from 1960 to 2010, and is expected to increase further by 1–5 °C by 2100 (Piao et al. 2010). Northern China is warming more than twice as fast as southern China. In addition, winter warming (0.04 °C per year) was found to be more pronounced than summer warming (0.01 °C per year) (Piao et al. 2010). Climate models also predict larger climatic variability and more frequent extreme events (e.g. droughts, storms and heat waves) in the future (Dong et al. 2011). A more variable *PPT* regime is likely to occur in the future, being characterized by more extreme rainfall events punctuated by longer intervening dry periods (Thomey et al. 2011). Particularly,

northern China is expected to experience increases in drought frequency and intensity (Liu and Feng 2012). Increases in both the severity and duration of drought are expected to profoundly impact ecosystem structure and functioning (Jongen et al. 2011; Biederman et al. 2016).

China is among the countries undergoing the most severe desertification, with the total desertification-affected area (2.62 million $km^2$) accounting for 27% of the national land area (Yang et al. 2005). China has made enormous effort in ecological restoration in arid and semiarid regions, as demonstrated by a series of ecological engineering projects carried out in northern China to combat desertification (Li et al. 2004). To date, restored vegetation covers more than 2.4 million hectares of degraded land in China (Gao et al. 2012). Endemic shrub species are widely used in this vast region for restoration, as they effectively reduce wind erosion (Wang et al. 2014). Revegetated shrublands can also serve to simultaneously sequester carbon for mitigating climate change and increase forage production (Gao et al. 2012). Significant shrubland expansion has been observed in northern China (Zhang et al. 2016). Shrub ecosystems in these areas are particularly susceptible to environmental perturbations and human activities (Gao et al. 2012). Considering the large extent of arid and semiarid ecosystems in China, changes in desertification-affected area may have significant effects on the global carbon balance and climate change (Poulter et al. 2014; Ahlström et al. 2015).

Shrubland ecosystems at the southern edge of the Mu Us Desert (also referred to as the Mu Us Sandland) lie in a critical geographical transition zone between arid and semiarid climates, and between agricultural and pastoral land uses. From the mid-20th century, human disturbances, especially overgrazing and inadequate reclamation, have caused severe vegetation degradation and desertification problems in this area (Chen and Duan 2009). Grazing on natural shrublands and steppes has been prohibited since the late 1990s, and large-scale rehabilitation practices (fencing and revegetation with shrubs) have been put into action (Chen and Duan 2009). Therefore, the vegetation has been given the opportunity to recover for almost two decades. The reversal of desertification has been evidenced by increases in vegetation cover and species diversity, increasingly fine soil texture, increased soil nutrient contents and reduced wind erosion (Chen and Duan 2009). In particular, the growth and expansion of xerophytic shrub species (e.g. *Artemisia ordosica* (Compositae), *Hedysarum mongolicum* (Leguminosae) and *Hedysarum scoparium* (Leguminosae)) have been found in the restoring area of the Mu Us Desert.

Based on both *in situ* measurements and model simulations, shrublands are shown to play an important role in maintaining ecosystem functions in northern China (Bourque and Hassan 2009; Zhang et al. 2016). However, little has been done to quantify the carbon sequestration potential of the recovering shrub vegetation (Gao et al. 2012; Liu et al. 2016). In addition, few (if any) studies have formally examined the biophysical control of surface energy partitioning (e.g. the evaporative fraction, $EF$, and the Bowen ratio, $\beta$) and the associated bulk surface parameters (e.g. bulk surface conductance, $g_s$; the decoupling coefficient, $\Omega$; and the Priestley-Taylor coefficient, $\alpha$) in these shrub-dominated ecosystems. In order to reduce uncertainties in predicting regional and global ecosystem functioning under a warming climate, it is necessary to understand how exchanges of carbon, water and energy between the biosphere and atmosphere in dry areas respond to current climatic variability (Gao et al. 2012; Biederman et al. 2016; Liu et al. 2016). These issues are essential to the evaluation of current rehabilitation efforts and to adaptive ecosystem management under a changing climate.

### 1.2 Biophysical controls on carbon, water and energy exchange

Whether and when an ecosystem is a net sink or source of $CO_2$ is affected by the way it responds to variability in driving environmental factors (Liu et al. 2012). In semiarid and arid ecosystems, moisture-related factors such as *PPT*, soil water content (*SWC*) and vapor pressure deficit (*VPD*) usually exert strong influences on diurnal, seasonal and interannual variations in the net ecosystem $CO_2$ exchange (*NEE*) (Fu et al. 2006; Gao et al. 2012). Water deficit may depress gross ecosystem production (*GEP*) by limiting physiological processes (e.g. stomatal closure) and altering plant phenology (e.g. delayed leaf emergence) and canopy structure (e.g. reduced leaf area index, *LAI*) (Zhou et al. 2013). Low water availability may also limit total ecosystem respiration (*TER*) by reducing root activity, microbial decomposition of organic matter and the diffusion of extra-cellular enzymes and carbon substrates in the soil (Wang et al. 2014). Moreover, the effects of water availability on *GEP* and *TER* depend not only on the sensitivity of related biotic processes and the magnitude of water stress but also on the temporal pattern of water supply. For example, *NEE* in dryland ecosystems showed inconsistent responses to rainfall events (Liu et al. 2011; Gao et al. 2012), indicating our lack of understanding on how dryland ecosystems respond to water stress and its relief. The role of abiotic stresses and their alleviation may play a more important role in regulating carbon cycling in the face of an increasing frequency and intensity of extreme climatic events in the future (Jongen et al. 2011; Thomey et al. 2011).

Besides water availability, *NEE* in arid and semiarid ecosystems is also affected by other abiotic and biotic factors. Drought stress is often accompanied with thermal and irradiation stresses, as the cloudiness is usually low and the soil is readily heated up by solar radiation during dry periods. High leaf temperature can deactivate photosystem II, enhance the evaporative demand for plants and stimulate respiration (Fu et al. 2006). Strong irradiation is common in arid and semiarid areas, and is likely to induce photosynthetic depression at midday (Fu et al. 2006). In many ecosystems, canopy development or phenology is critical to the seasonal evolution of $CO_2$ fluxes (Xu and Baldocchi 2004; Li et al. 2005). However, the large stochasticity of *PPT* and variability of soil moisture in arid and semiarid ecosystems can obscure the effects of *LAI* (Wang et al. 2008). Considering the inconsistent effects of these environmental stresses and biotic factors on $CO_2$ fluxes (e.g. Fu et al. 2006; Aires et al. 2008a; Wang et al. 2008), further studies are needed to examine the relative importance of these biophysical controls and their interactions at different timescales in desert shrub ecosystems.

The response of ecosystem energy partitioning to climate change is a major concern to ecologists and climate scientists because of local and regional feedbacks to climate, which in turn affects ecosystem carbon and water cycles (Aires et al. 2008b; Krishnan et al. 2012; Launiainen et al. 2016). Evapotranspiration (*ET*), which corresponds to the latent heat flux ($\lambda E$), is closely linked to ecosystem productivity (Aires et al. 2008b). The energy exchange between the biosphere and the atmosphere involves complex interactions among environmental (e.g. solar radiation, temperature and moisture) and biological (e.g. plant functional type, phenology and stomatal regulation) factors (Ding et al. 2013; Tang et al. 2014). The relative roles of biophysical variables can vary among ecosystem types (Aires et al. 2008b; Li et al. 2009; Krishnan et al. 2012). For example, in mesic forests and grasslands, shoot growth strongly controls energy partitioning via its impact on eco-physiological processes (e.g. transpiration), surface albedo and roughness (Hammerle et al. 2008). In boreal coniferous forests, low radiation and temperature are key factors

limiting the energy dissipated as $\lambda E$ (Launiainen 2010). In contrast, arid and semiarid areas are characterized by sporadic *PPT*, sparse vegetation and dry soils (Li et al. 2006). In such environments, the spatio-temporal variability of water availability strongly affects the dynamics of surface energy exchange (Li et al. 2006). In general, previous studies have not yet produced a consistent functional pattern for the responses of energy partitioning (e.g. *EF* and $\beta$) and bulk canopy parameters (e.g. $g_s$ and $\Omega$) to biophysical controls in arid and semiarid areas (Ding et al. 2013). Therefore, a better understanding of the biophysical controls on energy partitioning in these ecosystems is required for a proper assessment of regional and global carbon budget under changing climate (Li et al. 2006; Krishnan et al. 2012). In particular, the determination of major factors affecting energy partitioning can help predict how dryland ecosystems will respond to climatic variability and extremes (e.g. increases in drought duration and frequency) (Baldocchi and Xu 2007). Measurements of the seasonal trends of bulk canopy parameters and their biophysical controls for water-limited vegetation can be further used to better parameterize and validate eco-hydrological models (Krishnan et al. 2012; Ding et al. 2013; Launiainen et al. 2016).

Knowledge on the key factors affecting annual ecosystem production and water use efficiency (*WUE*) in dryland areas is crucial to the projection of global carbon balance under changing climate. Previous studies showed that semiarid grasslands and steppes have larger interannual variability in carbon and water exchange than forest and grassland ecosystems in mesic areas, and that semiarid ecosystems could switch from a net carbon sink in wet or normal years to a carbon source in dry years (Aires et al. 2008a; Jongen et al. 2011; Scott et al. 2015; Liu et al. 2016). Although water is considered a key factor affecting ecosystem carbon and water exchange in dryland regions, the response of ecosystem production to year-to-year fluctuations in *PPT* often varies among sites (Sala et al. 2012; Scott et al. 2015). Many previous studies have suggested that annual *PPT* amount is a good predictor of annual *NPP*, net ecosystem production (*NEP*) or *GEP* (Huxman et al. 2004; Scott et al. 2015; Biederman et al. 2016). However, some other studies have showed weak or non-significant relationships between annual *PPT* and ecosystem production (Xu and Baldocchi 2004; Gilmanov et al. 2006; Jongen et al. 2011; Sala et al. 2012). This inconsistency contrasts with the usually tight spatial relationships between mean annual precipitation (*MAP*) and *NPP*, *NEP* or *GEP* found by global and regional data syntheses (Huxman et al. 2004; Bai et al. 2008; Xiao et al. 2013). Clearly, the relationship between interannual variations in *PPT* and ecosystem production remains to be clarified for arid and semiarid areas.

Slight changes to the amount and timing of *PPT* may also trigger a complex interaction of physical, chemical and biological processes at the ecosystem level (Liu et al. 2011). The seasonal pattern of *PPT* can be more important than its total amount in determining the annual carbon balance in semiarid ecosystems (Jongen et al. 2011; Liu et al. 2016). Hydrologic losses through runoff and evaporation may also render *PPT* amount inaccurate as a measure of water availability for eco-physiological processes (Scott et al. 2015; Biederman et al. 2016). In addition, carry-over effects from the earlier year may further complicate the responses of annual ecosystem production to *PPT* (Sala et al. 2012).

*WUE* is a critical link between carbon and water cycling (Niu et al. 2011). Ecosystem *WUE* tends to increase with increasing *MAP* at the regional scale (Bai et al. 2008; Xiao et al. 2013). However, Huxman et al. (2004) reported an opposite trend in rain use efficiency (*RUE*) across a broader *MAP* gradient (i.e. data from throughout North and South America). Evidence based on individual sites often lacks consensus on the response of *WUE* to drought. Previous studies have shown either increases (Huxman et al. 2004; Bai et al. 2008;

Dong et al. 2011) or decreases (Liu et al. 2012; Scott et al. 2015) in *WUE* during dry years. The organizational level of aggregation (e.g. leaf, canopy or ecosystem), the way *WUE* is computed (e.g. *NPP*/*PPT*, *GEP*/*ET* or *NEP*/*ET*), or the timescale of analysis (e.g. seasonal, interannual and multi-decadal) may have contributed to the observed inconsistent drought effects on *WUE* and carbon exchange (Bai et al. 2008; Niu et al. 2011; Scott et al. 2015). Thus, a better understanding is needed of the relationship between year-to-year variations in water availability and ecosystem *WUE*, which can help constrain predictions of carbon and water coupling under changing climate. In addition, information on how key eco-physiological parameters (e.g. maximum carbon uptake rate and $g_s$) respond to interannual variations in climatic factors can help improve the modeling of carbon and water cycles.

### 1.3 Objectives of the study

The main aim of this study was to investigate the dynamics and biophysical controls of carbon, water and energy exchange over a semiarid shrub ecosystem in the Mu Us desert, northern China, using continuous eddy-covariance (EC) measurements. Specific objectives were as follows:

(1) To examine intra-annual variations in net ecosystem $CO_2$ exchange (*NEE)* and its biophysical controls (Paper I).
(2) To quantify the diurnal and seasonal variations in surface energy-balance components, and to examine the partitioning of net radiation ($R_n$) among different energy components at diurnal and seasonal timescales (Paper II).
(3) To examine how ecosystem production and water use efficiency (*WUE)* varied inter-annually with contrasting precipitation (*PPT*) and soil moisture patterns (Paper III).

The hypotheses tested in this study were as follows:
(1) Soil water shortage is dominant factor over other stress factors in controlling *NEE* of dryland ecosystems and could modify the responses of *NEE* to other environmental factors (Paper I).
(2) Seasonal dynamics of leaf area index (*LAI*) is an important determinant of productivity over the growing season, whereas abiotic stresses constrain $CO_2$ fluxes at shorter timescales (e.g. hourly to daily) (Paper I).
(3) Soil moisture and canopy phenology exert the most important controls over energy partitioning as mediated by bulk surface conductance ($g_s$) (Paper II).
(4) Decreases in water availability, which is determined by the amount and seasonal pattern of *PPT*, reduce gross ecosystem productivity (*GEP)* more than total ecosystem respiration (*TER)* and evapotranspiration *(ET)*, leading to lower net ecosystem production (*NEP)* and *WUE* (Paper III).

# 2. MATERIALS AND METHODS

## 2.1 Study site

This study was conducted at the Yanchi Research Station (37°42’31”N, 107°13’37”E, 1530 m a.s.l.) of Beijing Forestry University. The site is located in Ningxia, Northwest China, and lies at the southern edge of the Mu Us Desert, an area of mid-temperate semiarid continental climate (Fig. 1). The mean annual air-temperature (1954–2004) is 8.1 °C, with mean monthly temperature ranging from -8.7 °C in January to 22.4 °C in July (Chen and Duan 2009; Wang et al. 2014). The *MAP* of 287 mm is much lower than pan-evaporation (2024 mm). In addition, *PPT* shows large seasonal (~80% of annual amount falls during June–September) and interannual variation (145–587 mm). The growing season (May–October) is usually warm and receives most of the annual *PPT*. The soil is sandy with a bulk density of 1.54 ± 0.08 g cm-3 (mean ± SD, $n$ = 16) in the upper 10 cm of the soil profile. The studied shrubland is dominated by a mixture of xerophytic shrub species, including *A. ordosica* (35% relative cover), *H. mongolicum* (30%), *H. scoparium* and *Salix psammophila* (Salicaceae) (20%), with a minor component (15% percent cover) of grass species such as *Stipa capillata* (Gramineae) and *Agropyron cristatum* (Gramineae). The shrub canopy is about 1–1.5 m tall. Shrub roots are distributed mainly in the 20–50 cm soil layer. Soil water availability depends entirely on *PPT* as the water table lies 8–10 m below the ground surface. Seasonal water deficit constrains plant photosynthesis and soil respiration of the studied shrub ecosystem (Feng et al. 2013; Wang et al. 2014).

## 2.2 EC and meteorological measurements

An EC tower was established in June 2011 at Yanchi Research Station for measuring carbon, water and energy fluxes in a typical recovering shrubland ecosystem at the southern

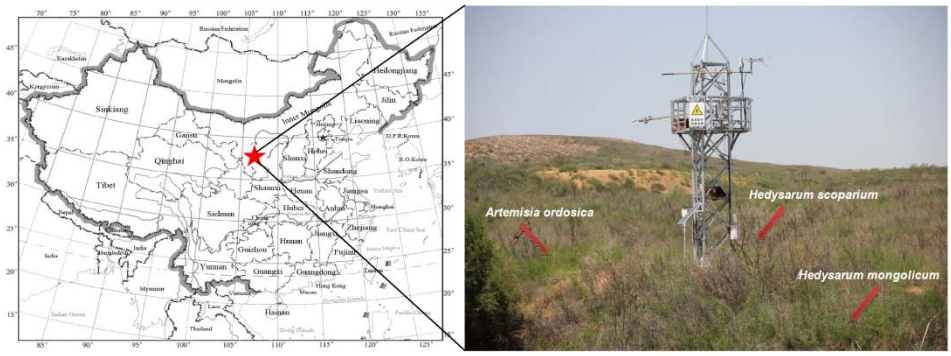


**Figure 1**. Location of the study site (left), the studied shrubland and the eddy-covariance tower (right).

edge of the Mu Us Desert. The EC system, which consists of an ultrasonic anemometer and an infrared gas analyzer, was mounted at a height of 6.2 m on a scaffold tower. A 3D ultrasonic anemometer (CSAT3, Campbell Scientific Inc., USA) was used to measure fluctuations in wind speed, direction and sonic temperature. A closed-path fast response infrared gas analyzer (LI-7200, LI-COR Inc., USA) was used to measure fluctuations in $CO_2$ and water vapor ($H_2O$) concentrations. Raw signals were recorded at 10 Hz using a data logger (LI-7550, LI-COR Inc., USA).

Incident photosynthetically active radiation (*PAR*) was measured using a quantum sensor (PAR-LITE, Kipp & Zonen, The Netherlands). $R_n$ was measured using a four-component radiometer (CNR-4, Kipp & Zonen, The Netherlands). Air temperature ($T_a$) and relative humidity were measured with a thermohygrometer (HMP155A, Vaisala, Finland). Wind speed ($u$) and direction was measured with a wind set (034B, Met One Instruments Inc., USA). All these meteorological sensors were mounted on the tower at 6 m above the ground. Half-hourly soil temperature ($T_s$) and water content (*SWC*) were measured at four depths (10, 30, 70 and 120 cm) within 10 m of the tower, with three replicate sensors ($ECH_2O$-5TE, Decagon Devices, USA) at each depth. Soil heat flux ($G$) was calculated as the sum of the heat flux at 10-cm depth, measured within 10 m of the tower using five soil heat flux transducers (HFP01, Hukseflux Thermal Sensors, The Netherlands), and the rate of change in heat storage in the soil layer above the transducers (Ochsner et al. 2007). Rainfall was measured daily with a manual rain gauge from 15 May to 22 July 2012, and thereafter with a tipping-bucket rain gauge (TE525WS, Campbell Scientific Inc., USA) at a distance of ~50 m from the tower. Daily rainfall values from 1 January to 14 May 2012 measured at the nearest weather station (37°48'N, 107°23'E, 1349 m a.s.l., ~20 km from the study site) were included to obtain the total rainfall amount in 2012. Details on instrumentation and sampling procedures can be found in Paper I and II.

## 2.3 Data processing and analysis

### *2.3.1 Flux calculation, quality control and gap-filling*

Raw $CO_2$ and $H_2O$ records were processed using the EddyPro 4.0.0 software (LI-COR Inc., USA), through steps including spike removal, double coordinate rotation, time delay corrections, frequency response corrections, detrending (block averaging) and flux computation (Burba 2013). The Webb-Pearman-Leuning (WPL) correction was not required because the LI-7200 outputs the $CO_2$ and $H_2O$ mixing ratio directly, i.e. thermal expansion and water dilution of the sampled air have already been accounted for (Burba 2013). $CO_2$ and $H_2O$ fluxes were also excluded from analyses when turbulent mixing was low during calm nights (friction velocity $u^* < 0.18$ m s$^{-1}$). The $u^*$ filtering, however, was not applied to turbulent energy fluxes (i.e. $\lambda E$ and sensible heat flux, $H$). Half-hourly carbon, water and energy fluxes were despiked following Papale et al. (2006). Positive values for turbulent fluxes denote transfer of $CO_2$, $H_2O$ and energy upwards to the atmosphere (i.e. source). Paper I and II provide more details on flux calculation and quality control.

Instrument failure and maintenance resulted in 3%, 16% and 5% missing $CO_2$ and $H_2O$ flux records in 2012, 2013 and 2014, respectively; while the quality control procedure discarded 26%, 21% and 26% of annual $CO_2$ and $H_2O$ flux values for 2012–2014. Instrument failure, maintenance and data screening together caused 5%, 17% and 7% missing $\lambda E$ values for 2012–2014, compared to 2%, 17% and 6% missing $H$ values for the

three years. Missing $R_n$ or $G$ values never exceeded 2% for each of the three years.

All missing values were replaced with estimated values in order to calculate the annual carbon, water and energy budgets. Linear interpolation was used to fill small gaps (≤ 2 h). For larger gaps in $CO_2$ time series during daytime (i.e. $PAR \geq 5$ μmol photons $m^{-2}$ $s^{-1}$), empirical *NEE–PAR* relationships were used for gap-filling. A light response model (refer to Paper I and III, Eq. 1,) which was modified from the rectangular hyperbola to incorporate photoinhibition at high radiation was used to estimate missing daytime *NEE* ($NEE_{day}$) because net $CO_2$ uptake declined at high *PAR*, especially in summer. The light response model was fit to consecutive windows of 500 non-missing daytime data points to obtain seasonally-varying parameter values.

To estimate missing nighttime *NEE* values ($NEE_{night}$), an exponential function was fit to the relationship between half-hourly $NEE_{night}$ and soil temperature at the 10-cm depth ($T_{s\_10}$) for each year. The exponential function was only fit to the annual dataset because short-term data points were too scattered to establish any valid $NEE_{night}$–$T_s$ relationships. Therefore, model parameters for *TER* did not vary seasonally.

Missing values in the independent variables (*PAR* and $T_{s\_10}$) of these functions were estimated using either the mean diurnal variation (MDV) method (Falge et al. 2001) or empirical relationships with other micro-meteorological measurements (e.g. global solar radiation and $T_a$). Daytime *TER* during the growing season was extrapolated from the temperature response function for $NEE_{night}$. *TER* during the non-growing season was considered equal to *NEE*. *GEP* was then estimated as *TER* minus *NEE*. See Paper I for a detailed description of the procedure for filling gaps in $CO_2$ fluxes.

Missing $\lambda E$ and $H$ flux values were filled following a similar procedure to that described by Amiro et al. (2006). In brief, nighttime missing $\lambda E$ values were set to zero. Daytime missing $\lambda E$ values were estimated by the regression between $\lambda E$ and $R_n - G$ for good daytime data periods, based on a 240-point (half-hour period) moving window, moved in an increment of 48 points at a time. Missing $H$ values were estimated by the regression between $H$ and $R_n - G$, using a similar moving window approach. Remaining gaps in $\lambda E$ and $H$ time series (due to missing $R_n$ or $G$) were filled by applying the MDV method to consecutive 15-day windows.

### *2.3.2 Calculation of canopy and ecosystem parameters*

Bulk surface parameters, including the surface conductance ($g_s$, m $s^{-1}$), decoupling coefficient ($\Omega$) and Priestley-Taylor coefficient ($\alpha$), were calculated to help investigate the biophysical controls on $\lambda E$ and *NEE* (see Paper II and III for details). The surface conductance ($g_s$) was estimated by inverting the Penman-Monteith equation (Monteith 1965). The value of $g_s$ represents the aggregate conductance of dry canopy (transpiration), wet canopy (evaporation) and soil surface (evaporation). However, during the growing season when *ET* in semiarid ecosystems originates largely from transpiration, $g_s$ strongly reflects the canopy-integrated stomatal conductance (Liu and Feng 2012).

The decoupling coefficient ($\Omega$) was calculated following Jarvis and McNaughton (1986). $\Omega$ is a measure of the degree of coupling between the ecosystem surface and the atmospheric boundary layer. $\Omega$ varies from 0 (i.e. canopy surface and the atmosphere are coupled and $\lambda E$ is mostly controlled by $g_s$ and *VPD*) to 1 (i.e. canopy surface and the atmosphere are decoupled and $\lambda E$ is mostly controlled by $R_n$).

The coefficient $\alpha$ is the ratio of actual $\lambda E$ to the equilibrium $\lambda E$ ($\lambda E_{eq}$) (Aires et al. 2008b). The $\lambda E_{eq}$ was estimated following Priestley and Taylor (1972). Usually, $\alpha \geq 1$ can

be expected in mesic ecosystems, indicating sufficient water supply so that $\lambda E$ is limited by available energy (Launiainen 2010). In contrast, $\alpha < 1$ has been observed in semiarid and arid ecosystems where $\lambda E$ is usually water-limited (Liu and Feng 2012). Low $\alpha$ values in dryland ecosystems can result from stomatal control on transpiration and/or scarce water supply to soil evaporation (Launiainen et al. 2016).

Energy partitioning (*EF*, i.e. $\lambda E/R_n$ and $\beta$, i.e. $H/\lambda E$) and bulk surface parameters ($g_s$, $\Omega$ and $\alpha$) were calculated for dry canopy periods only (non-rainy days) since these periods are most pertinent to understandings of biophysical controls on energy partitioning. To avoid spurious values caused by low solar elevation, all periods when shortwave incoming radiation was less than 100 W $m^{-2}$ were rejected (Li et al. 2006). See Paper II for a detailed description of the calculation of canopy and ecosystem parameters.

Following Huemmrich et al. (1999) and Wilson and Meyers (2007), the tower-based normalized-difference vegetation index (*NDVI*) was calculated with incident and reflected radiation measurements for *PAR* and global solar radiation (Paper III). After Beer et al. (2009), *WUE* at the ecosystem level was calculated as the ratio of *GEP* to *ET*, or as the slope of the *GEP* vs. *ET* relationship; while the inherent *WUE* (*IWUE*) was calculated as ecosystem *WUE* multiplied by the mean daytime *VPD* (i.e. the ratio of $GEP \cdot VPD$ to *ET*), or as the slope of the ($GEP \cdot VPD$) vs. *ET* relationship. The *IWUE* used here can be considered an analogue of leaf-level *IWUE* (i.e. the ratio of photosynthesis rate to stomatal conductance) at the ecosystem level (Beer et al. 2009).

### *2.3.3 Uncertainty analysis*

The cumulative effects of random measurement uncertainty in annual *NEP* and *ET* were evaluated with the successive days approach (Hollinger and Richardson 2005; Dragoni et al. 2007) (see Paper I and III for details). This method infers the statistical properties of the random error from the difference between half-hourly flux measurements made exactly 24 h apart. The effects of imperfect environmental similarity between the successive days were controlled for following Dragoni et al. (2007). A Monte Carlo approach was then used to generate a random error for each measured half-hourly flux value. The simulation was repeated 2000 times and the uncertainty of the measured annual *NEP* or *ET* were estimated by calculating the 90% prediction limits or standard deviation of all simulated annual flux values. Similarly, the random uncertainties for annual *GEP* and *TER* were evaluated following a Monte Carlo algorithm detailed by Hagen et al. (2006). The algorithm infers the statistical properties of the random error from the residuals of the model for gap-filling and flux partitioning. Again, the 90% prediction limits or standard deviation of all ($N$ = 2000) simulated annual *GEP* and *TER* values were calculated. The resulting *GEP* and *TER* uncertainties encompass sources from both measurement error and model parameterization (Hagen et al. 2006).

### *2.3.4 Statistical analysis*

To evaluate the seasonal variation in light response of *NEE*, a modified rectangular hyperbolic model (Eq. (1) in Paper I and III) was fit monthly from May to October. The model was fit to bin-averaged data (50 μmol $m^{-2}$ $s^{-1}$ *PAR* bins). In order to test the dependency of the $NEE_{day}$–*PAR* relationship on abiotic factors and exclude the confounding effects of plant phenology, $NEE_{day}$ during the peak growing season (Jun–Aug) was complied into multiple groups according to *VPD*, $T_a$ and *SWC* at 30 cm depth (Paper I). The

$NEE_{day}$ values were then bin-averaged before parameters were fit for each group. To evaluate the relative importance of different abiotic factors, the light-response model was fit to all half-hourly $NEE_{day}$ values during June–August, and the residuals were then subjected to least-square regressions and a stepwise multiple linear regression against *VPD*, $T_a$ and *SWC*. In order to test $NEE_{day}$–$T_a$ and $NEE_{day}$–*VPD* relationships, as well as their dependency on *SWC*, $NEE_{day}$ was compiled with respect to *SWC* at 30 cm depth (*SWC*_30 ≤ 0.1 $m^3$ $m^{-3}$, *SWC*_30 > 0.1 $m^3$ $m^{-3}$), and then bin-averaged into 1 °C $T_a$ and 0.2 kPa *VPD* intervals, respectively. $NEE_{day}$–$T_a$ and $NEE_{day}$–*VPD* relationships were fit with the quadratic model. Soil moisture at 30 cm depth was used in all analyses because its effects were most pronounced among *SWC* at different layers. In addition, this layer corresponds to the main rooting depth (20–50 cm) of the dominant shrub species at the site (Wang et al. 2015).

To examine the effects of *SWC* on the *TER*–$T_{s\_10}$ relationship, $NEE_{night}$ when $T_{s\_10}$ > 0 °C was classified into two groups with respect to *SWC*_30 (*SWC*_30 ≤ 0.1 $m^3$ $m^{-3}$, *SWC*_30 > 0.1 $m^3$ $m^{-3}$), and then bin-averaged $NEE_{night}$ into 1 °C $T_{s\_10}$ intervals (Paper I). An exponential model was fit to $NEE_{night}$ vs. $T_{s\_10}$ separately for each *SWC* group. A surface fitting was then used to further examine the interaction between temperature and water availability in regulating half-hourly $NEE_{night}$.

Regression analyses were also used to test the effects of *LAI*, *SWC*_30 and *VPD* on *EF*, $\alpha$, $g_s$, $\Omega$ and $\beta$, and to examine the role of $g_s$ in controlling *EF*, $\alpha$ and $\Omega$ (Paper II). Response variables were bin-averaged before regressions were conducted. For testing the effects of abiotic controls (*SWC*_30 and *VPD*), only data from the mid-growing season (June–August) were used to minimize the confounding effects of canopy phenology. The effects of $g_s$ were assessed for both the whole year and the mid-growing season using bin-averaged values (0.5 mm $s^{-1}$ $g_s$ intervals).

Path analysis was used to elucidate the direct and indirect effects of biophysical factors (*LAI*, *SWC*_30, *VPD*, $T_a$ and $g_s$) on *EF* and $\alpha$ (Paper II). The direct path coefficient between two variables is the standardized partial-regression coefficient (which varies from -1 to 1) given by multiple regression, and the indirect path coefficient is the product of direct coefficients summed over all paths. The total path coefficient is the sum of direct and indirect coefficients. Initial models included all potential causalities based on widely accepted knowledge, and final models were derived by removing insignificant ($p \geq 0.05$) paths and recalculating coefficients.

Linear fitting was used to test relationships between some variables of interest (e.g. *GEP* vs. *LAI*, *TER* vs. *GEP*, *GEP* vs. *ET*) (Paper I and III). Analysis of Covariance (ANCOVA) was performed to test for significant year-to-year differences in the intercept (the main effect of year) and slope (year × *ET* interaction) of regression lines of *GEP* or (*GEP* · *VPD*) vs. *ET* (Paper III). Separate lines for each year were reported where the intercept and/or slope differed significantly among years. Otherwise, a common line was fit to the pooled data. For the nonlinear relationship between *WUE* and *VPD*, a common curve for the pooled data was reported as fit parameters for separate curves showed overlapping 95% confidence intervals (i.e. non-significant differences).

# 3. RESULTS

## 3.1 Temporal variation in biophysical factors

The seasonal patterns of $T_a$, $T_{s\_10}$, incident *PAR* and *VPD* were similar among the three years (See Paper III, Table 1 and Fig. 1). Daily mean $T_a$ ranged from about -8 °C in winter to 25 °C in summer. Daily incident *PAR* had minimum values (<5 mol $m^{-2}$ $day^{-1}$) on cloudy winter days and maximums (~60 mol $m^{-2}$ $day^{-1}$) in summer. *VPD* was slightly lower in 2012 than the following two years.

The three years were characterized by contrasting seasonal patterns of *PPT* and *SWC* (See Paper III, Fig. 1). Annual rainfall was higher in 2014 (19% above *MAP*) and 2012 (17% above *MAP*) than 2013 (3% below *MAP*). Significant interannual differences in *SWC* were also noticeable in spring. Soil thaw caused a step rise in *SWC*_30 in early spring, followed by a gradual depletion until *SWC*_30 was recharged by the first significant rain event. Spring *SWC*_30 showed sustained high values in 2012 and sustained low values in 2014. At the study site, little rain or snow occurs from late autumn to early-spring, so that early-spring *SWC*_30 following soil thaw was similar to the values from the preceding autumn. *SWC* at 10-cm depth (*SWC*_10) was more affected by small rain events and surface drying than *SWC*_30, which responded mainly to rainfall events larger than 20 mm $day^{-1}$.

Clear seasonal cycles were observed for tower-based *NDVI* and *LAI* (See Paper I and III, Fig. 1). Canopy development was generally in phase with solar irradiance and the wet period. The seasonal maximum of *NDVI* was higher in 2012 (0.47) and 2013 (0.47) than 2014 (0.37). Moreover, 2012 and 2013 had a mean *NDVI* of 0.38 for the carbon uptake period (i.e. daily $GEP > 0$), compared to 0.28 in 2014. A decreasing trend was observed in both the seasonal maximum and the growing-season mean of $g_s$ from 2012 to 2014 (See Paper III, Fig. 1).

## 3.2 Temporal dynamics of carbon, water and energy exchange

Diurnal variations in *NEE* were first examined for the year 2012 (Paper I, Fig. 10). The monthly mean diurnal variations showed that the diel amplitude of *NEE* was largest in July and smallest in October. Net $CO_2$ uptake showed an asymmetric pattern around noon on summer days (June–August), peaking at 09:30–10:00 LST (GMT + 8). *PAR* showed a symmetric diurnal pattern, whereas both $T_a$ and *VPD* were lowest in early morning and peaked in late afternoon. Comparison of the mean diurnal variations among the three years (2012–2014) revealed dramatic interannual differences in both *NEE* and *ET* during the early- to mid-growing season (May and July), when daytime carbon uptake, nighttime carbon release and *ET* were all highest in 2012 and lowest in 2014 (Paper III, Fig. 3). The diurnal courses of both *NEE* and *ET* were similar among years during the late growing season (September). Diurnal variations in energy fluxes were also examined for 2012 (Paper II, Fig. 5). The midday maximum $R_n$ ranged from about 250 W $m^{-2}$ in January to over 500 W $m^{-2}$ in July. The diurnal peaks of *H* and *G* varied from about 190 and 50 W $m^{-2}$ in winter to 250 and 140 W $m^{-2}$ in spring, respectively. $\lambda E$ was close to zero during winter, while displayed a clear diurnal cycle during the growing season, with a maximum diurnal

peak of 180 W $m^{-2}$ in July. During midday (10:00–15:00), *H* was generally larger than $\lambda E$ in most months except July, when $\lambda E$ exceeded *H*.

The three years differed markedly in the seasonal and annual patterns of carbon and water fluxes (Paper III, Table 1; Fig. 2). Daily *NEE* varied in the range -4.71 to 1.63, -2.38 to 2.13 and -2.11 to 1.51 g C $m^{-2}$ $day^{-1}$ in 2012–2014, respectively (negative values indicate net carbon uptake). Maximum daily *GEP* was 6.78 g C $m^{-2}$ $day^{-1}$ (DOY 182) in 2012, 4.63 g C $m^{-2}$ $day^{-1}$ (DOY 203) in 2013 and 3.21 g C $m^{-2}$ $day^{-1}$ (DOY 243) in 2014. Although the carbon uptake period was of similar length (DOY 115–302) across the three years, the number of carbon sink days (i.e. daily $NEE < 0$) varied, being 131, 122 and 113 days for 2012–2014, respectively. Daily *TER* was low in winter (<0.5 g C $m^{-2}$ $day^{-1}$), and had seasonal peaks of 3.26, 2.76 and 2.02 g C $m^{-2}$ $day^{-1}$ in 2012–2014, respectively. The shrubland was a moderate carbon sink in 2012 ($NEP = 77 \pm 10$ g C $m^{-2}$ $yr^{-1}$), almost carbon neutral in 2013 (-4 ± 10 g C $m^{-2}$ $yr^{-1}$), but switched to a weak carbon source in 2014 (-22 ± 5 g C $m^{-2}$ $yr^{-1}$). Annual *TER* was less variable than *GEP* among years, although both of them were highest in 2012 and lowest in 2014. Maximum *ET* was 3.4, 3.6 and 2.5 mm $day^{-1}$ for the three years, respectively. Annual *ET* was highest in 2012 (282 ± 3 mm) and lowest in 2014 (194 ± 2 mm). Daily *WUE* during the growing season varied between 1–4 g C $kg^{-1}$ H2O. The dry soil conditions in the spring of 2014 led to markedly suppressed *WUE* till early August. Annual *WUE* was similar in 2012 and 2013, but declined in 2014.

In 2012, the seasonal course of daily $R_n$ ranged from less than 1 MJ $m^{-2}$ $day^{-1}$ in winter to over 15 MJ $m^{-2}$ $day^{-1}$ in summer (Paper II, Fig. 2). Cumulative $R_n$ over the year was 2548 MJ $m^{-2}$. Daily *G* varied from negative values in late autumn and winter (a minimum of -2.4 MJ $m^{-2}$ $day^{-1}$) to about 2 MJ $m^{-2}$ $day^{-1}$ in spring and early summer. Daily *H* showed a bimodal seasonal pattern, with a spring peak of 11.3 MJ $m^{-2}$ $day^{-1}$ on 25 May (DOY 116) and an autumn plateau of about 6.5 MJ $m^{-2}$ $day^{-1}$ during DOY 220–270. *H* was low during wintertime (~2 MJ $m^{-2}$ $day^{-1}$). Cumulative *H* over the year was 1411 MJ $m^{-2}$, and the annual $H/R_n$ was 0.55. Daily $\lambda E$ was smaller than 1 MJ $m^{-2}$ $day^{-1}$ throughout the winter, increased from spring to mid-summer (with a maximum of 7.9 MJ $m^{-2}$ $day^{-1}$), and declined thereafter. In addition, $\lambda E$ was greater than *H* only during a short period in early summer (DOY 170–220). The annual sum of $\lambda E$ was 695 MJ $m^{-2}$, corresponding to an annual *EF* of 0.27. The dry-canopy *EF* and bulk surface parameters ($\alpha$, $g_s$ and $\Omega$) showed similar seasonal trends in 2012 (Paper II, Fig. 4). Their daily mean values were generally close to zero during wintertime, but reached a maximum ($EF = 0.6$, $\alpha = 0.9$, $g_s = 7.7$ mm $s^{-1}$ and $\Omega = 0.6$) in late June or early July.

### 3.3 Biophysical controls on carbon, water and energy exchange

As expected, *PAR* had strong influences on $NEE_{day}$ during the growing season. However, the effect of *PAR* was modified by other environmental factors (Paper I, Fig. 3). The magnitude of the maximum rate of net $CO_2$ uptake ($NEE_{max}$) decreased with increasing *VPD* and $T_a$. In addition, the magnitude of both $NEE_{max}$ and the average daytime ecosystem respiration ($R_d$) were lower under dry soil conditions. $NEE_{night}$ related positively with $T_{s\_10}$ cm depth for both *SWC*_30 groups (Paper I, Fig. 5). However, the temperature sensitivity of $NEE_{night}$ ($Q_{10}$) was much larger, with the rate of $NEE_{night}$ at 10 °C ($R_{e10}$) slightly smaller, for the higher *SWC*_30 group. Surface regression showed that $Q_{10}$ increased from 1.9 to 3.2, and $R_{e10}$ increased with from 0.73 to 0.83 μmol $CO_2$ $m^{-2}$ $s^{-1}$, as the relative extractable water (*REW*) increased from 0 to 1 (Paper I, Fig. 6).

The light response curve of $NEE_{day}$ varied both seasonally and among years (Paper III, Fig. 4). $NEE_{max}$ showed a unimodal seasonal pattern, peaking in July 2012, July 2013 and August–September 2014. A delayed peak in 2014 was also found for the quantum yield. $NEE_{max}$ in spring and summer was smaller in 2013 than 2012, and $NEE_{max}$, initial quantum yield and $R_d$ were all much lower in 2014 than the previous two years. However, all parameters converged to similar values towards the end of the growing season. $NEE_{night}$ increased exponentially with $T_{s\_10}$ when $T_{s\_10}$ was lower than 20 °C. $NEE_{night}$ plateaued or declined slightly with further increases in $T_{s\_10}$. Above the tipping point, $NEE_{night}$ was highest in 2012 and lowest in 2014 (Paper III, Fig. 5).

In 2012, daily *TER* was linearly related to *GEP*, with a slope of 0.34 (Paper I, Fig. 8a). Both daily *GEP* and *NEE* responded linearly to the seasonal variation of *LAI*, with a slope of 4.12 and -2.03, respectively (Paper I, Fig. 8b, c). Daily *GEP* linearly increased daily *ET*, with highest slope observed in 2012 and lowest in 2014 (Paper III, Fig. 6). Bin-averaged half-hourly *WUE* decreased with increasing *VPD* (Paper III, Fig. 7a). The *WUE–VPD* relationship was not significantly different among the three years and was well described by a common exponential function.

In 2012, seasonal variations in *LAI* significantly affected *EF* and bulk surface parameters (Paper II, Fig. 6). During the mid-growing season (June–August), *EF*, $g_s$ $\alpha$ and $\Omega$ were all strongly correlated with *SWC*_30 (Paper II, Fig. 7). Both *EF* and $\alpha$ increased with *VPD* up to *VPD* values of 1 kPa, but then leveled off to *EF* and $\alpha$ asymptotes of about 0.38 and 0.6, respectively (Paper II, Fig. 8). Bin-averaged $g_s$ increased slightly with *VPD* up to *VPD* of 1 kPa, then decreased from a peak of 5 mm $s^{-1}$ to about 2 mm $s^{-1}$ at *VPD* of 3 kPa. Bin-averaged $\Omega$ showed a strong negative correlation with *VPD*. *EF*, $\alpha$ and $\Omega$ were all tightly and positively correlated with $g_s$ (Paper II, Fig. 10).

Path analysis (Paper II, Fig. 11) revealed strong positive effects of $g_s$ on *EF* and $\alpha$, with the direct path coefficients exceeding 0.90. High *VPD* also directly promoted *EF* and $\alpha$, with a direct path coefficient of 0.52. *LAI* was the main factor controlling $g_s$, followed by *SWC* and *VPD* whose direct effects on $g_s$ were similar in magnitude but opposite in sign. In addition, high *VPD* indirectly suppressed $g_s$, via a negative effect on *SWC*_30. As mediated by $g_s$, the indirect path coefficients of *LAI*, *SWC* and *VPD* on *EF* ($\alpha$) were 0.68 (0.66), 0.30 (0.29) and -0.36 (-0.35), respectively. The indirect effects of *VPD* partially offset its direct effects, resulting in a total path coefficient of 0.16 for *EF* and 0.17 for $\alpha$. Neither *LAI* nor *SWC* showed any significant direct effect on *EF* and $\alpha$, their total path coefficients therefore equaled indirect path coefficients.

# 4. DISCUSSION AND CONCLUSIONS

## 4.1 Evaluation of methodology

This study used the EC technique to investigate the dynamics and biophysical controls of carbon, water and energy exchange over a semiarid shrub ecosystem in the Mu Us desert, northern China. Based on continuous EC measurements, intra-annual variations in net ecosystem $CO_2$ exchange (*NEE*) and its biophysical controls were examined using measurements throughout 2012 (Paper I). Data for 2012 were then analyzed to quantify the diurnal and seasonal variations in surface energy-balance components, and to examine how $R_n$ was partitioned among different energy components at diurnal and seasonal timescales

(Paper II). Finally, measurements for three years (2012–2014) with contrasting *PPT* and soil moisture patterns were analyzed to examine the how ecosystem production and water use efficiency (*WUE*) vary inter-annually (Paper III).

Although the EC technique is considered more accurate and reliable than traditional methods (e.g. chambers, biomass inventory) in quantifying ecosystem carbon balance (Baldocchi 2003), several methodological issues need to be addressed here. Firstly, the overall performance of the EC measurements was assessed by the degree of energy balance closure. Annual energy balance closure as indicated by the slope of the relationship between turbulent energy ($\lambda E$ and $H$) and available energy ($R_n - G$) varied from 74% in 2014 to 82% in 2012. This range falls within that (0.53–0.99 with a mean of 0.79) reported for FLUXNET sites (Wilson et al. 2002), indicating that measurements in this study are reliable. As in most previous studies, energy-closure adjustments were not applied to EC fluxes because of the unclear cause of energy imbalance (Wilson et al. 2002). Secondly, storage flux terms in the air column below the EC instrument height were not added to estimates of *NEE* and *ET*. Calculation of the storage terms for $\lambda E$ and $H$ following Zha et al. (2004) revealed that aboveground energy storage terms contributed negligibly to the surface energy closure. This finding indicates that *NEE* and *ET* values estimated without their respective aboveground storage terms are reliable. Small storage flux terms resulted from the short-statured canopy (1–1.5 m) and a low sensor height, which usually render storage terms negligible (Zhang et al. 2007). In addition, the cumulative storage terms should get close to zero as the timescale increases (e.g. daily, seasonal and annual) (Baldocchi 2003; Burba 2013). Thirdly, the underlying surface of the shrubland was flat and extended over 250 m in all directions. Footprint analysis using the flux source area model (FASM) (Schmid 1997) showed that >90% of the fluxes originated from within 200 m of the tower. Therefore, the study site met the requirements by the EC technique in terms of topography and fetch. Lastly, data gaps were few (see 2.3.1) during the study period (2012–2014) and occurred mostly in the non-growing season, ensuring reliability of the results.

## 4.2 Evaluation of results

### *4.2.1 Temporal dynamics of carbon, water and energy exchange and their biophysical controls*

The total amount of carbon sequestered by the studied shrubland in 2012 (*NEP* = 77 ± 10 g C $m^{-2}$ $yr^{-1}$) (Paper I), with an annual rainfall of 335 mm (48 mm higher than MAP) and a peak *LAI* of 1.2 $m^2$ $m^{-2}$ (equivalent to a maximum *NDVI* of 0.47), was generally lower than that sequestered by forests and grasslands in humid and subhumid areas (e.g. Suyker and Verma 2001; Zha et al. 2004; Zhou et al. 2013). However, the *NEP* observed in 2012 was higher than many reported values from semiarid and arid non-forest ecosystems (Wang et al. 2008; Gao et al. 2012). For example, a revegetated shrub ecosystem ~200 km west of the studied shrubland dominated by *Caragana korshinskii* (Leguminosae) and *A. ordosica* had a *NEP* of 14–23 g C $m^{-2}$ $yr^{-1}$, with an annual *PPT* of <150 mm (Gao et al. 2012). An semiarid steppe in central Mongolia showed a *NEP* of 41 g C $m^{-2}$ $yr^{-1}$, with an annual *PPT* of 260 mm and a peak *LAI* of 0.57 (Li et al. 2005). *NEP* in the studied shrubland reduced to -4 ± 10 g C $m^{-2}$ in 2013 and further to -22 ± 5 g C $m^{-2}$ in 2014 (Paper III), probably as a result of year-to-year variations in *PPT* and soil moisture. Based on this study, the broad distribution of arid and semiarid shrublands in north and northwest China represents a

considerable carbon fixation potential at the regional scale, as long as an adequate water supply is provided.

The relative magnitude of different energy-balance components varied with time of year and the timescale considered in 2012 (Paper II). Sensible heat (*H*) was the dominant term on an annual basis (i.e. with an annual $\beta$ of 2.0), and *H* exceeded $\lambda E$ during most of the year. Similar $\beta$ values have been reported for other arid and semiarid ecosystems where low *PPT*, dry soils and a sparse canopy constrain $\lambda E$ (Li et al. 2006; Hao et al. 2007; Aires et al. 2008b). Daily $\lambda E$ dominated *H* during the mid-summer of 2012 when rainfall was frequent and *LAI* was high. The inverse relationship between $\lambda E$ and *H* over the growing season is consistent with previous observations in semiarid steppe and shrub ecosystems (Li et al. 2006). An annual *EF* of 0.27 was close to that (0.26) reported by Li et al. (2006), and fell within the range (0.18–0.29) reported for an undisturbed semiarid grassland in North America (Krishnan et al. 2012). However, it was lower than that in a Mediterranean C3/C4 grassland (0.37–0.45) (Aires et al. 2008b) and in a typical steppe in northern China (0.39–0.42) (Hao et al. 2007). Low *EF* may be characteristic of shrub ecosystems in northern China due to their arid climate and sparse vegetation.

Water stress, which varies significantly at hourly to seasonal scales, is the most common limitation to vegetation growth in dryland ecosystems (Fu et al. 2006). Results of this study supported the hypothesis that soil water shortage plays a dominant role in limiting photosynthesis, and could modify the responses of $NEE_{day}$ to other environmental factors (Paper I). Findings of this study that low *SWC*_30 and high *VPD* depressed the maximum rate of $CO_2$ uptake ($NEE_{max}$) were in agreement with previous studies in dryland ecosystems (Li et al. 2005; Wang et al. 2008; Yang et al. 2011). Both *SWC*_30 and *VPD* affect plant hydraulic status, however, they reduce carbon assimilation through partially different mechanisms. Dry soil leads to reduced water supply for metabolism and cell expansion, while drought-related increases in *VPD* affect $CO_2$ supply for photosynthesis by regulating stomatal conductance and evaporative demand (Zhou et al. 2013). In this study, these two mechanisms did not act in isolation, but interacted to reduce $CO_2$ uptake under water-stressed conditions. Li et al. (2005) suggested that the sensitivity of stomata to *VPD* becomes stronger once leaf water potential starts to drop because of deficient water supply from the soil. Low soil water availability may aggravate *VPD*-induced stomatal closure.

Water limitation to ecosystem or soil respiration has been found in various types of ecosystems (Gao et al. 2012). This study showed a marked decrease in both the magnitude and $Q_{10}$ of *TER* under low *SWC*_30 (Paper I). The reduction in $Q_{10}$ of *TER* under drought conditions was most likely associated with decreased carbon transportation to roots due to suppressed photosynthesis, deactivated rhizosphere and switched carbon pool being respired (e.g. from labile to recalcitrant) (Zhang et al. 2007; Wang et al. 2008; Gao et al. 2012).

This study found that *LAI* accounted for 45% and 65% of the seasonal variation in *NEE* and *GEP* in 2012, respectively, supporting the hypothesis that canopy development is an important determinant of productivity over the growing season (Paper I). The effects of leaf area on *NEE* and *GEP* lie in the role that leaves play in determining the amount of photosynthetic tissues and the amount of intercepted light by the vegetation (Yang et al. 2011). Similar *GEP–LAI* and *NEE–LAI* relationships have been reported for steppe, grassland and pasture ecosystems (e.g. Tappeiner and Cernusca 1998, Flanagan et al. 2002; Yang et al. 2011). The slope of the *GEP–LAI* relationship reported here (4.1 g C $m^{-2}$ leaf area $day^{-1}$) was comparable to that in a semiarid steppe (3.1 g C $m^{-2}$ $day^{-1}$) (Li et al. 2005) and two Mediterranean grasslands (3.9-4.1 g C $m^{-2}$ $day^{-1}$, Xu and Baldocchi 2004; Aires et

al. 2008a). However, it was much smaller than that found in a Canadian temperate grassland (7.5–8.7 g C $m^{-2}$ $day^{-1}$, Flanagan et al. 2002). A small *GEP–LAI* slope may be indicative of water and nutrient limitations (Li et al. 2005).

Results of this study support the hypothesis that water availability and canopy development are the primary factors affecting $\lambda E$ in semiarid shrub ecosystems (Paper II). Although there was a synchrony between the supply and demand for water, $\lambda E$ was often moisture-limited due to limited *PPT*. During the mid-growing season, $\beta$ decreased exponentially with soil moisture, which is consistent with previous studies (Bracho et al. 2008). *EF* ($\alpha$) increased linearly from 0.30 (0.45) under dry conditions (*SWC*_30 = 0.06 $m^3$ $m^{-3}$) to 0.5 (0.7) under wet conditions (*SWC*_30 = 0.16 $m^3$ $m^{-3}$). In addition, the linear dependence of $g_s$ and $\Omega$ on *SWC*_30 suggested a strong stomatal control on *ET* and a tight canopy-atmosphere coupling under dry conditions (Li et al. 2006; Liu and Feng 2012). These results are in line with previous studies of semiarid grasslands, shrublands and steppes (Baldocchi et al. 2004; Li et al. 2006; Aires et al. 2008b; Krishnan et al. 2012).

Canopy structure and *LAI* regulate energy partitioning via their impacts on surface albedo, roughness and stand transpiration (Li et al. 2006; Hammerle et al. 2008). Consistent with previous studies in semiarid steppes and grasslands (e.g. Li et al. 2006; Hao et al. 2007; Krishnan et al. 2012), this study showed that *LAI* affected the seasonality of energy partitioning and bulk canopy parameters (Paper II). In addition, the monthly reference $g_s$ at *VPD* of 1 kPa followed the seasonal pattern of *LAI*, indicating that canopy phenology acted in concert with environmental factors to control the seasonal cycle of $\lambda E$.

The tight relationships of *EF* and $\alpha$ with $g_s$ observed in this study are consistent with previous studies (Li et al. 2007; Krishnan et al. 2012; Liu and Feng 2012), and indicate strong eco-physiological regulation of energy partitioning and *ET* in the studied shrubland (Paper II). These relationships together with the path analyses supported the hypothesis that $g_s$ strongly and directly affected energy partitioning and bulk canopy parameters. Moreover, neither *SWC*_30 nor *LAI* showed any significant direct effect on *EF* and $\alpha$; but their controlling effects were mediated through $g_s$. Based on this study, the energy partitioned to $\lambda E$ was largely controlled by the phenology of *LAI* and environmental regulation on $g_s$.

### *4.2.2 Effects of precipitation timing and soil moisture carry-over on ecosystem productivity*

*PPT* strongly affects the structure and functioning of semiarid ecosystems (Huxman et al. 2004; Sala et al. 2012). Annual *PPT* amount has been identified as an important factor driving interannual variations in *NPP*, *NEP* and *WUE* for forests and grasslands (e.g. Aires et al. 2008a; Bai et al. 2008; Dong et al. 2011; Biederman et al. 2016). However, this study found that the year with the highest rainfall (2014, 342 mm) during the study period showed the lowest ecosystem production and *WUE*, and that annual *PPT* could not explain year-to-year variations in ecosystem fluxes (e.g. *NEP*, *GEP*, *TER* and *ET*) and *WUE*. There are also some studies that found weak or non-significant relationships between annual total *PPT* and ecosystem production (Sala et al. 2012; Liu et al. 2015). More significant than annual total *PPT* is usually the seasonal pattern of *PPT* (e.g. Gilmanov et al. 2006; Kwon et al. 2008; Jongen et al. 2011; Zhou et al. 2013).

Annual total *PPT* is not always an accurate metric of the water available to drive plant and soil $CO_2$ cycling (Scotts et al. 2015; Biederman et al. 2016). This has been reported for arid and semiarid ecosystems in different regions around the world (Jongen et al. 2011; Sala et al. 2012; Liu et al. 2016). Firstly, small rain events rarely recharge the soil moisture at plant rooting depth, although they may trigger increased microbial respiration in shallow

soil layers (Thomey et al. 2011). Previous studies at the same site found that roots of the dominant shrubs are mainly distributed in the 20–50 cm soil layer (Wang et al. 2015), and seasonal variations in *NEE* were strongly regulated by *SWC* at 30-cm depth, rather than that at a shallower (10-cm) depth. The present study showed that higher annual carbon and water fluxes corresponded to higher spring *SWC*_30 and that *SWC*_30 did not respond to the large number of small rainfall events (i.e. <20 mm $day^{-1}$). Multiple small rain events in the spring of 2014 failed to alleviate the detrimental effects of low initial *SWC*_30. It has been proposed that even for a given total annual *PPT*, different seasonal patterns, e.g. frequent intermediate and small events vs. less frequent but larger events, may have contrasting effects on plant water uptake, growth and ecosystem productivity (Thomey et al. 2011).

Secondly, eco-physiological processes may depend on water availability during particular phenophases, leading to the decoupling of total *PPT* quantity and plant water demand (Dong et al. 2011; Liu et al. 2016). At the study site, low springtime soil moisture was associated with suppressed seasonal and annual ecosystem production. Ample rainfall in the summer and autumn of 2014 did not completely offset the adverse impacts of spring dry soil conditions, although late-season *NEP* and its light-response parameters had recovered to levels comparable to those in 2012 and 2013. Similarly, late *PPT* events have been found to result in smaller proportional increases in *GEP* than early events (Jongen et al. 2011; Zhou et al. 2013). A recent analysis on nine years of EC data also found that *PPT* during pre-growing season (November–April), rather than annual total or growing-season *PPT*, played an important role in controlling ecosystem productivity (Liu et al. 2016).

Thirdly, hydrologic losses (i.e. through surface runoff, deep drainage and evaporation) may decouple *PPT* from soil water available for biotic $CO_2$ exchange (Biederman et al. 2016). Recent synthesis studies on ecosystem responses to climatic variability suggest the use of *ET* as a proxy for the amount of water available to ecosystem production (Scott et al. 2015; Biederman et al. 2016). Results of this study support this view, showing that low productivity years were associated with low *ET*, irrespective of annual *PPT*.

This study found that low soil moisture conditions in spring coincided with lower seasonal and annual carbon and water fluxes, as well as lower *WUE*. Spring drought may affect ecosystem productivity through different mechanisms. Firstly, water deficit during the early growing season has been reported to hinder leaf emergence and canopy development, resulting in reduced leaf area index (*LAI*) (Aires et al. 2008a; Dong et al. 2011). In the studied shrubland, *NDVI* was lower in 2014 than in previous two years, likely a result of the severe spring drought in 2014. Secondly, dry air and/or soil conditions may induce partial stomatal closure of dominant shrub species, as indicated by suppressed growing-season $g_s$, which reflects the canopy-integrated stomatal conductance. Reduced *LAI* combined with stomatal closure can lead to suppressed canopy photosynthetic capacity (Yang et al. 2013; Liu et al. 2016). Thirdly, annual *GEP* has been proposed to be jointly controlled by photosynthetic capacity and plant phenology (Xia et al. 2015). However, the decreases in *GEP* in years with low spring soil moisture found in this study were largely attributable to suppressed canopy photosynthetic capacity, as the carbon uptake period remained unchanged across years. Finally, community composition has been shown to be an important driver of ecosystem productivity in response to interannual variations in *PPT* (Liu et al. 2016). In the studied shrubland, the relative abundance of dominant species did not change much during the measurement period, so that shifts in community composition are not expected to account for observed patterns in carbon and water fluxes.

Drought events may affect *GEP* and *TER* differently, thus modifying *NEP* (Zhou et al.

2013). Results of this study are in line with the previous hypothesis that *GEP* is more sensitive than *TER* to spring drought in semiarid shrublands and steppes (Kwon et al. 2008; Dong et al. 2011; Niu et al. 2011). However, short-term drought may suppress *TER* more than *GEP* because heterotrophic respiration is controlled by shallow *SWC* in the litter and upper soil layers, which dry first, whereas photosynthesis is affected by moisture that is accessible to roots in deeper soil layers (Reichstein et al. 2002; Yang et al. 2013). Therefore, the interaction among the timing, severity and duration of drought should be considered when comparing the sensitivities of *GEP* and *TER* to water stress.

*GEP* and *ET* may also show different sensitivities to spring drought, leading to changes in *WUE*. This study found that lower annual *WUE* and shallower slope of the *GEP* vs. *ET* relationship occurred in years characterized by dry spring soil conditions. Findings of this study are consistent with previous studies in semiarid areas showing stronger drought impact on *GEP* than *ET* (Aries et al. 2008a; Niu et al. 2011; Liu et al. 2012). It is worth mentioning that despite decreases in ecosystem-level *WUE*, leaf- and canopy-level *WUE* (e.g. the ratio of assimilation to transpiration) may remain unaffected or even increase in response to water stress, as stomatal closure limits $H_2O$ loss more than $CO_2$ assimilation (Dong et al. 2011; Liu et al. 2012). Therefore, the level of biological organization should be explicitly considered when modeling and interpreting *WUE* responses to drought (Niu et al. 2011).

*PPT* legacy effects (i.e. effects of past *PPT* on current ecosystem properties) may simply result from the carry-over of soil moisture between years (Sala et al. 2012). At the study site, little soil water recharge occurred from late autumn to early-spring, so that early-spring *SWC*_30 was similar to the values from the preceding autumn. Therefore, years preceded by low late-season *PPT* may undergo spring drought, negatively affecting annual ecosystem productivity and *WUE*. Results of this study are in line with previous findings that low winter/spring *PPT* led to inadequate recharge of deep soil moisture, and thus constrained growing-season *GEP* and *NEP* in semiarid steppe and shrubland ecosystems (Kwon et al. 2008; Liu et al. 2016). Alternatively, *PPT* legacy effects may be mediated by structural (e.g. biomass, density, *LAI* and species composition) or biogeochemical (e.g. litter input and nutrient availability) changes (Sala et al. 2012). Long-term studies at the site are needed to investigate how drought-induced structural and biogeochemical changes (e.g. decreases in *NDVI* as a result of the severe spring drought in 2014) may influence ecosystem productivity and *WUE* in the following year.

### 4.3 Conclusions

Based on three years of EC measurements, this study investigated the carbon, water and energy exchange over a semi-arid shrubland in northern China. Water stress (e.g. high *VPD*) exerted a strong control over half-hourly fluctuations in *NEE* during the peak growing season, and interacted with heat stress and photoinhibition in constraining carbon fixation. Rain pulses regulated *NEE* at the synoptic scale, highlighting the role of water supply in the alleviation of abiotic stresses. Canopy development largely determined the dynamics of *NEE* and *GEP* over the entire growing season. Inter-annual variations in water availability had large impacts on carbon sequestration of the shrub-dominated ecosystem, causing it to switch rapidly between an annual sink and source of $CO_2$. Spring soil moisture deficit reduced seasonal and annual *GEP* more than *TER* or *ET*, leading to decreases in carbon sequestration and *WUE*. Little soil moisture recharge occurred during winter, so that spring

soil moisture following soil thaw resulted from the legacy of the preceding year's water balance. *ET* may be a better proxy than *PPT* for water availability in order to predict carbon exchange on an annual basis. *H* was the primary energy-balance component in the studied shrub ecosystem, and $\lambda E$ exceeded *H* only during the mid-growing season. The $g_s$ imposed a dominant and direct control over $\lambda E$. Both water availability and canopy development were important factors effecting $g_s$, and thus increases in *SWC* and *LAI* enhanced $\lambda E$ indirectly.

Results of this study highlight the role of abiotic stresses and their alleviation in regulating carbon cycling in the face of an increasing frequency and intensity of extreme climatic events. The results also indicate the importance of adaptive plant responses to water scarcity in regulating ecosystem carbon, water and energy exchange. *PPT* timing and soil moisture carry-over may play an important role in controlling ecosystem productivity. These findings may apply to the vast areas of desert shrublands and steppes in northern China due to their broad climatic, edaphic and vegetation similarities.

The present study has important implications for projecting ecosystem responses to climate change. Climate modeling suggests a warmer and drier future climate in the semiarid and arid regions of Asia (McCarthy et al. 2001; Piao et al. 2010). Hence, more stressful environmental conditions in the future may lead to substantially lower carbon sequestration capacity in temperate semiarid areas. Also, the predicted higher variability in *PPT* (Easterling et al. 2000; Thomey et al. 2011), i.e. more extreme but less frequent rainfall events intervened by longer dry periods, accentuates the role of the temporal pattern of water availability in controlling *NEE* in the future. Throughout China, the past decades have witnessed a faster rate of warming in winter than summer, a trend that is expected to continue (Piao et al. 2010). Increases in air and soil temperatures during winter can lead to shorter soil-freezing periods, higher evaporative water losses, and thus lower carry-over of soil moisture for springtime leaf emergence and expansion. Climate models predict changes in both the amount and variability of PPT (Thomey et al. 2011). The observed trend of decreasing autumn/winter *PPT* in northern China (Liu et al. 2005; Piao et al. 2010), even under constant or increased annual *PPT*, could intensify spring drought and thus impair the carbon sequestration potential of semi-arid shrubland and steppe ecosystems.

## REFERENCES

Ahlström A., Raupach M.R., Schurgers G., Smith B., Arneth A., Jung M., Reichstein M., Canadell J.G., Friedlingstein P., Jain A.K., Kato E., Poulter B., Sitch S., Stocker B.D., Voivy N., Wang Y.P., Wiltshire A., Zaehle S., Zeng N. (2015). The dominant role of semi-arid ecosystems in the trend and variability of the land $CO_2$ sink. Science 348: 895–899.
http://dx.doi.org/10.1126/science.aaa1668

Aires L.M.I., Pio C.A., Pereira J.S. (2008a). Carbon dioxide exchange above a Mediterranean C3/C4 grassland during two climatologically contrasting years. Global Change Biology 14: 539–555.
http://dx.doi.org/10.1111/j.1365-2486.2007.01507.x

Aires L.M., Pio C.A., Pereira J.S. (2008b). The effect of drought on energy and water vapor exchange above a mediterranean C3/C4 grassland in Southern Portugal. Agricultural and Forest Meteorology 148: 565–579.
http://dx.doi.org/10.1016/j.agrformet.2007.11.001

Amiro B.D., Barr A.G., Black T.A., Iwashita H., Kljun N., McCaughey J.H., Morgenstern K., Murayama S., Nesic Z., Orchansky A.L., Saigusa N. (2006). Carbon, energy and water fluxes at mature and disturbed forest sites, Saskatchewan, Canada. Agricultural and Forest Meteorology 136: 237–251.
http://dx.doi.org/10.1016/j.agrformet.2004.11.012

Asner G.P., Archer S., Hughes R.F., Ansley R.J., Wessman C.A. (2003). Net changes in regional woody vegetation cover and carbon storage in Texas Drylands, 1937–1999. Global Change Biology 9: 316–335.
http://dx.doi.org/10.1046/j.1365-2486.2003.00594.x

Bai Y., Wu J., Xing Qi., Pan Q., Huang J., Yang D., Han X. (2008). Primary production and rain use efficiency across a precipitation gradient on the Mongolian Plateau. Ecology 89: 2140–2153.
http://dx.doi.org/10.1890/07-0992.1

Baldocchi D.D., Xu L. (2007). What limits evaporation from Mediterranean oak woodlands–The supply of moisture in the soil, physiological control by the plants or the demand by the atmosphere? Advances in Water Resources 30: 2113–2122.
http://dx.doi.org/10.1016/j.advwatres.2006.06.013

Baldocchi D.D. (2003). Assessing the eddy covariance technique for evaluating carbon dioxide exchange rates of ecosystems: past, present and future. Global Change Biology 9: 479–492.
http://dx.doi.org/10.1046/j.1365-2486.2003.00629.x

Baldocchi D.D., Xu L., Kiang N. (2004). How plant functional-type, weather, seasonal drought, and soil physical properties alter water and energy fluxes of an oak-grass

savanna and an annual grassland. Agricultural and Forest Meteorology 123: 13–39. http://dx.doi.org/10.1016/j.agrformet.2003.11.006

Beer C., Ciais P., Reichstein M., Baldocchi D., Law B.E., Papale D., Soussana J.F., Ammann C., Buchmann N., Frank D., Gianelle D., Janssens I.A., Knohl A., Köstner B., Moors E., Roupsard O., Verbeeck H., Vesala T., Williams C.A., Wohlfahrt G. (2009). Temporal and among-site variability of inherent water use efficiency at the ecosystem level. Global Biogeochemical Cycles 23: GB2018. http://dx.doi.org/10.1029/2008GB003233

Biederman J.A., Scott R.L., Goulden M.L., Vargas R., Litvak M.E., Kolb T.S., Yepez E.A., Oechel W.C., Blanken P.D., Bell T.W., Garatuza-Payan J., Maurer G.E., Bore S., Burns S.P. (2016). Terrestrial carbon balance in a drier world: the effects of water availability in southern North America. Global Change Biology 22: 1867–1879. http://dx.doi.org/10.1111/gcb.13222

Bourque C.P.A., Hassan Q.K. (2009). Vegetation control in the long-term self-stabilization of the Liangzhou Oasis of the upper Shiyang River. Earth Interactions 13: 13. http://dx.doi.org/10.1175/2009EI286.1

Bracho R., Powell T.L., Dore S., Li J., Hinkle C.R., Drake B.G. (2008). Environmental and biological controls on water and energy exchange in Florida scrub oak and pine flatwoods ecosystems. Journal of Geophysical Research 113: G02004. http://dx.doi.org/10.1029/2007JG000469

Burba G. (2013). Eddy Covariance Method for Scientific, Industrial, Agricultural and Regulatory applications. LI-COR Biosciences, Lincoln, USA.

Chen X., Duan Z. (2009). Changes in soil physical and chemical properties during reversal of desertification in Yanchi County of Ningxia Hui autonomous regions, China. Environmental Geology 57: 975–985. http://dx.doi.org/10.1007/s00254-008-1382-1

Ding R., Kang S., Li F., Zhang Y., Tong L. (2013). Evapotranspiration measurement and estimation using modified Priestley-Taylor model in an irrigated maize field with mulching. Agricultural and Forest Meteorology 168: 140–148. http://dx.doi.org/10.1016/j.agrformet.2012.08.003

Dong G., Guo J., Chen J., Sun G., Gao S., Hu L., Wang Y. (2011). Effects of spring drought on carbon sequestration, evapotranspiration and water use efficiency in the Songnen Meadow Steppe in Northeast China. Ecohydrology 4: 211–224. http://dx.doi.org/10.1002/eco.200

Dragoni D., Schmid H.P., Grimmond C.S.B., Loescher H.W. (2007). Uncertainty of annual net ecosystem productivity estimated using eddy covariance flux measurements. Journal of Geophysical Research 112: D17102. http://dx.doi.org/10.1029/2006JD008149

Easterling D.R., Meehl G.A., Parmesan C., Changnon S.A., Karl T.R., Mearns L.O. (2000). Climate extremes: observations, modeling, and impacts. Science 289: 2068–2074. http://dx.doi.org/10.1126/science.289.5487.2068

Emanuel W.R., Shugart H.H., Stevenson M.P. (1985). Climate change and the broad scale distributions of terrestrial ecosystem complexes. Climate Change 7: 29–43. http://dx.doi.org/10.1007/BF00139439

Falge E., Baldocchi D., Olson R., Anthoni P., Aubinet M., Bernhofer C., Burba G., Ceulemans R., Clement R., Dolman H., Granier A., Gross P., Grünwald T., Hollinger D., Jensen N.O., Katul G., Keronen P., Kowalski A., Lai C.T., Law B.E., Meyers T., Moncrieff J., Moors E., Munger J.W., Pilegaard K., Rannik Ü., Rebmann C., Suyker A., Tenhunen J., Tu K., Verma S., Vesala T., Wilson K., Wofsy S. (2001). Gap-filling strategies for defensive annual sums of net ecosystem exchange. Agricultural and Forest Meteorology 107: 43–69. http://dx.doi.org/10.1016/S0168-1923(00)00225-2

Feng W., Zhang Y., Wu B., Zha T., Jia X., Qin S., Shao C., Liu J., Lai Z., Fa K. (2013). Influence of disturbance on soil respiration in biologically crusted soil during the dry season. The Scientific World Journal: Article ID 408560. http://dx.doi.org/10.1155/2013/408560

Field C., Behrenfeld M., Randerson J., Falkowski P. (1998). Primary production of the biosphere: integrating terrestrial and oceanic components. Science 281: 237–240. http://dx.doi.org/10.1126/science.281.5374.237

Flanagan L.B., Wever L.A., Carlson P.J. (2002). Seasonal and interannual variation in carbon dioxide exchange and carbon balance in a northern temperate grassland. Global Change Biology 8: 599–615. http://dx.doi.org/10.1046/j.1365-2486.2002.00491.x

Fu Y.L., Yu G.R., Sun X.M., Li Y.N., Wen X.F., Zhang L.M., Li Z.Q., Zhao L., Hao Y.B. (2006). Depression of net ecosystem $CO_2$ exchange in semi-arid *Leymus chinensis* steppe and alpine shrub. Agricultural and Forest Meteorology 137: 234–244. http://dx.doi.org/10.1016/j.agrformet.2006.02.009

Gao Y., Liu L., Jia R., Yang H., Li G., Wei Y. (2012). Seasonal variation of carbon exchange from a revegetation area in a Chinese desert. Agricultural and Forest Meteorology 156: 134–142. http://dx.doi.org/10.1016/j.agrformet.2012.01.007

Gilmanov T.G., Svejcar T.J., Johnson D.A., Angell R.F., Saliendra N.Z., Wylie B.K. (2006). Long-term dynamics of production, respiration, and net $CO_2$ exchange in two Sagebrush-steppe ecosystems. Rangeland Ecology and Management 59: 585–599. http://dx.doi.org/10.2111/05-198R1.1

Hagen S.C., Braswell B.H., Linder E., Frolking S., Richardson A.D., Hollinger D.Y. (2006). Statistical uncertainty of eddy flux-based estimates of gross ecosystem carbon

exchange at Howland Forest, Maine. Journal of Geophysical Research 111: D08S03. http://dx.doi.org/10.1029/2005JD006154

Hammerle A., Haslwanter A., Tappeiner U., Cernusca A., Wohlfahrt G. (2008). Leaf area controls on energy partitioning of a temperate mountain grassland. Biogeosciences 5: 421–431. http://dx.doi.org/10.5194/bg-5-421-2008

Hao Y. Wang Y., Huang X., Cui X., Zhou X., Wang S., Niu H., Jiang G. (2007). Seasonal and interannual variation in water vapor and energy exchange over a typical steppe in Inner Mongolia, China. Agricultural and Forest Meteorology 146: 57–69. http://dx.doi.org/10.1016/j.agrformet.2007.05.005

Hollinger D.Y., Richardson A.D. (2005). Uncertainty in eddy covariance measurements and its application to physiological models. Tree Physiology 25: 873–885. http://dx.doi.org/10.1093/treephys/25.7.873

Huemmrich K.F., Black T.A., Jarvis P.G. McCaughey J.H., Hall F.G. (1999). High temporal resolution NDVI phenology from micrometeorological radiation sensors. Journal of Geophysical Research 104: 27, 935–27, 944. http://dx.doi.org/10.1029/1999JD900164

Huxman T.E., Smith M.D., Fay P.A., Knapp A.K., Rebecca Shaw M., Loik M.E., Smith S.D., Tissue D.T., Zak J.C., Weltzin J.F., Pockman W.T., Sala O.E., Haddad B.M., Harte J., Koch G.W., Schwinning S., Small E.E., Williams D.G. (2004). Convergence across biomass to a common rain-use efficiency. Nature 429: 651–654. http://dx.doi.org/10.1038/nature02561

Jarvis P.G., McNaughton K.G. (1986). Stomatal control of transpiration: scaling up from leaf to region. Advances in Ecological Research 15: 1–49. http://dx.doi.org/10.1016/S0065-2504(08)60119-1

Jongen M., Pereira J.S., Aires L.M.J., Pio C.A. (2011). The effects of drought and time of precipitation on the inter-annual variation in ecosystem-atmosphere exchange in a Mediterranean grassland. Agricultural and Forest Meteorology 151: 595–606. http://dx.doi.org/10.1016/j.agrformet.2011.01.008

Kwon H., Pendall E., Ewers B.E., Cleary M., Naithani K. (2008). Spring drought regulates summer net ecosystem $CO_2$ in a sagebrush-steppe ecosystem. Agricultural and Forest Meteorology 148: 381–391. http://dx.doi.org/10.1016/j.agrformet.2007.09.010

Krishnan P., Meyers T.P., Scott R.L., Kennedy L., Heuer M. (2012). Energy exchange and evapotranspiration over two temperate semi-arid grasslands in North America. Agricultural and Forest Meteorology 153: 31–44. http://dx.doi.org/10.1016/j.agrformet.2011.09.017

Lal R. (2004). Carbon sequestration in dryland ecosystems. Environmental Management 33:

528–544.
http://dx.doi.org/10.1007/s00267-003-9110-9

Launiainen S. (2010). Seasonal and inter-annual variability of energy exchange above a boreal Scots pine forest. Biogeosciences 7: 3921–3940.
http://dx.doi.org/10.5194/bg-7-3921-2010

Launiainen S., Katul G.G., Kolari P., Lindroth A., Lohila A., Aurela M., Varlagin A., Grelle A., Vesala T. (2016). Do the energy fluxes and surface conductance of boreal coniferous forests in Europe scale with leaf area? Global Change Biology 22: 4096–4113.
http://dx.doi.org/10.1111/gcb.13497

Li S.G., Asanuma J., Eugster W., Kotani A., Liu J.J., Urano T., Oikawa T., Davaa G., Oyunbaatar D., Sugita M. (2005). Net ecosystem carbon dioxide exchange over grazed steppe in central Mongolia. Global Change Biology 11: 1941–1955.
http://dx.doi.org/10.1111/j.1365-2486.2005.01047.x

Li S.G., Eugster W., Asanuma J., Kotani A., Davaa G., Oyunbaatar D., Sugita M. (2006). Energy partitioning and its biophysical controls above a grazing steppe in central Mongolia. Agricultural and Forest Meteorology 137: 89–106.
http://dx.doi.org/10.1016/j.agrformet.2006.03.010

Li S.G., Asanuma J., Kotani A., Davaa G., Oyunbaatar D. (2007). Evapotranspiration from a Mongolian steppe under grazing and its environmental constraints. Journal of Hydrology 333: 133–143.
http://dx.doi.org/10.1016/j.jhydrol.2006.07.021

Li X.R., Ma F.Y., Xiao H.L., Wang X.P., Kim K.C. (2004). Long-term effects of revegetation on soil water content of sand dunes in arid regions of Northern China. J. Arid Environments 57: 1–16.
http://dx.doi.org/10.1016/S0140-1963(03)00089-2

Li Y., Zhou L., Xu Z., Zhou G. (2009). Comparison of water vapor, heat and energy exchanges over agricultural and wetland ecosystems. Hydrological Processes 23: 2069–2080.
http://dx.doi.org/10.1002/hyp.7339

Liu B., Xu M., Henderson M., Qi Y. (2005). Observed trends of precipitation amount, frequency, and intensity in China, 1960-2000. Journal of Geophysical Research 110: D08103.
http://dx.doi.org/10.1029/2004JD004864

Liu H., Feng J. (2012). Seasonal and interannual variations of evapotranspiration and energy exchange over different land surfaces in a semi-arid area of China. Journal of Applied Meteorology and Climatology 51: 1875–1888.
http://dx.doi.org/10.1175/JAMC-D-11-0229.1

Liu R., Li Y., Wang Q.X. (2011). Variations in water and $CO_2$ fluxes over a saline desert in western China. Hydrological Processes 26: 513–522. http://dx.doi.org/10.1002/hyp.8147

Liu R., Pan L.P., Jenerette G.D., Wang Q.X., Cieraad E., Li Y. (2012). High efficiency in water use and carbon gain in a wet year for a desert halophyte community. Agricultural and Forest Meteorology 162–163: 127–135. http://dx.doi.org/10.1016/j.agrformet.2012.04.015

Liu R., Cieraad E., Li Y., Ma J. (2016). Precipitation pattern determines the inter-annual variation of herbaceous layer and carbon fluxes in a phreatophyte-dominated desert ecosystem. Ecosystems 19: 601–614. http://dx.doi.org/10.1007/s10021-015-9954-x

Liu Y., Xiao J., Ju W., Zhou Y., Wang S., Wu X. (2015). Water use efficiency of China's terrestrial ecosystems and responses to drought. Scientific Reports 5: 13799. http://dx.doi.org/10.1038/srep13799

McCarthy J., Canziani O., Leary N., Dokken D.J., White K.S. (2001). Climate Change 2001: Impacts, Adaptation, and Vulnerability. Cambridge University Press, New York.

Monteith J.L. (1965). Evaporation and environment. In: Fogg G.E. (ed). The State and Movement of Water in Living Organisms. Academic Press, New York. P. 205–234.

Niu S., Xing X., Zhang Z., Xia J., Zhou X., Song B., Li L., Wan S. (2011). Water-use efficiency in response to climate change: from leaf to ecosystem in a temperate steppe. Global Change Biology 17: 1073–1082. http://dx.doi.org/10.1111/j.1365-2486.2010.02280.x

Ochsner T.E., Sauer T.J., Horton R. (2007). Soil heat storage measurements in energy balance studies. Agronomy Journal 99: 311–319. http://dx.doi.org/10.2134/agronj2005.0103S

Papale D., Reichstein M., Aubinet M., Canfora E., Berhofer C., Kutsch W., Longdoz B., Rambal S., Valentini R., Vesala T., Yakir D. (2006). Towards a standardized processing of Net Ecosystem Exchange measured with eddy covariance technique: algorithms and uncertainty estimation. Biogeosciences 3: 571–583. http://dx.doi.org/10.5194/bg-3-571-2006

Piao S., Ciais P., Huang Y., Shen Z., Peng S., Li J., Zhou L., Liu H., Ma Y., Ding Y., Friedlingsteinm P., Liu C., Tan K., Yu Y., Zhang T., Fang J. (2010). The impacts of climate change on water resources and agricultural in China. Nature 467: 43–51. http://dx.doi.org/10.1038/nature09364

Poulter B., Frank D., Ciais P., Myneni R.B., Andela N., Bi J., Beoquet G., Canadell J.G., Chevallier F., Liu Y.Y., Running S.W., Sitch S., van der Werf G.R. (2014). Contribution of semi-arid ecosystems to inter-annual variability of the global carbon cycle. Nature 509: 600–603.

http://dx.doi.org/10.1038/nature13376

Priestley C.H.B., Taylor R.J. (1972). On the assessment of surface heat flux and evaporation using large-scale parameters. Monthly Weather Review 100: 81–92. http://dx.doi.org/10.1175/1520-0493(1972)100<0081:OTAOSH>2.3.CO;2

Reichstein M., Tenhunen J.D., Roupsard O., Ourcival J., Rambal S., Miglietta F., Peressotti A., Pecchiari M., Tirone G., Valentini R. (2002). Severe drought effects on ecosystem $CO_2$ and $H_2O$ fluxes at three Mediterranean evergreen sites: revisions of current hypotheses? Global Change Biology 8: 999–1017. http://dx.doi.org/10.1046/j.1365-2486.2002.00530.x

Reynolds J.F., Smith D.M.S., Lambin E.F., Turner II B.L., Mortimore M., Batterbury S.P.J., Downing T.E., Dowlatabadi H., Fernández R.J., Herrick J.E., Huber-Sannwald E., Jiang H., Leemans R., Lynam T., Maestre F.T., Ayarza M., Walker B. (2007). Global desertification: building a science for dryland development. Science 316: 847–851. http://dx.doi.org/10.1126/science.1131634

Sala O.E., Gherardi L.A., Reichmann L., Jobbágy E., Peters D. (2012). Legacies of precipitation fluctuations on primary production: theory and data synthesis. Philosophical Transactions of the Royal Society B Biological Sciences 367: 3135–3144. http://dx.doi.org/10.1098/rstb.2011.0347

Scott R.L., Biederman J.A., Hamerlynck E.P., Barron-Gafford G.A. (2015). The carbon balance pivot point of southwestern U.S. semiarid ecosystems: Insights from the 21st century drought. Journal of Geophysical Research: Biogeosciences 120: 2612–2624. http://dx.doi.org/10.1002/2015JG003181

Schmid H.P. (1997). Experimental design for flux measurements: matching scales of observations and fluxes. Agricultural and Forest Meteorology 87: 179–200. http://dx.doi.org/10.1016/S0168-1923(97)00011-7

Suyker A.E., Verma S.B. (2001). Year-round observations of the net ecosystem exchange of carbon dioxide in a native tallgrass prairie. Global Change Biology 7: 279–289. http://dx.doi.org/10.1046/j.1365-2486.2001.00407.x

Tappeiner U., Cernusca A. (1998). Model simulation of spatial distribution of photosynthesis in structural differing plant communities in the Central Caucasus. Ecological Modelling 113: 201–223. http://dx.doi.org/10.1016/S0304-3800(98)00144-6

Tang Y., Wen X., Sun X., Zhang X., Wang H. (2014). The limiting effect of deep soil water on evapotranspiration of a subtropical coniferous plantation subjected to seasonal drought. Advances in Atmospheric Sciences 31: 385–395. http://dx.doi.org/10.1007/s00376-013-2321-y

Thomey M.L., Collins S.L., Vargas R., Johnson J.E., Brown R.F., Natvig D.O., Friggens

M.T. (2011). Effect of precipitation variability on net primary production and soil respiration in a Chihuahuan Desert grassland. Global Change Biology 17: 1505–1515. http://dx.doi.org/10.1111/j.1365-2486.2010.02363.x

Wang B., Zha T.S., Jia X., Wu B., Zhang Y.Q., Qin S.G. (2014). Soil moisture modifies the response of soil respiration to temperature in a desert shrub ecosystem. Biogeosciences 11: 259–268. http://dx.doi.org/10.5194/bg-11-259-2014

Wang B., Zha T., Jia X., Gong J.N., Wu B., Bourque C.P.A., Zhang Y., Qin S.G., Chen G.P., Peltola H. (2015). Microtopographic variations in soil respiration and its controlling factors vary with plant phenophases in a desert-shrub ecosystem. Biogeosciences 12: 5705–5714. http://dx.doi.org/10.5194/bgd-12-9465-2015

Wang, Y., Zhou, G., and Wang, Y., 2008. Environmental effects on net ecosystem $CO_2$ exchange at half-hour and month scales over *Stipa krylovii* steppe in northern China. Agricultural and Forest Meteorology 148: 714–722. http://dx.doi.org/10.1016/j.agrformet.2008.01.013

Wilson T.B., Meyers T.P. (2007). Determining vegetation indices from solar and photosynthetically active radiation fluxes. Agricultural and Forest Meteorology 144: 160–179. http://dx.doi.org/10.1016/j.agrformet.2007.04.001

Wilson K., Goldstein A., Falge E., Aubinet M., Baldocchi D., Berbigier P., Bernhofer C., Ceulemans R., Dolman H., Field C., Grelle A., Ibrom A., Law B.E., Kowalski A., Meyers T., Moncrieff J., Monson R., Oechel W., Tenhunen J., Valentini R., Verma S. (2002). Energy balance closure at FLUXNET sites. Agricultural and Forest Meteorology 113: 223–243. http://dx.doi.org/10.1016/S0168-1923(02)00109-0

Wohlfahrt G., Fenstermaker L.F., Arnone III J.A. (2008). Large annual net ecosystem $CO_2$ uptake of a Mojave Desert ecosystem. Global Change Biology 14: 1475–1487. http://dx.doi.org/10.1111/j.1365-2486.2008.01593.x

Xiao J., Sun G., Chen J., Chen H., Chen S., Dong G., Gao S., Guo H., Guo J., Han S., Kato T., Li Y., Lin G., Lu W., Ma M., McNulty S., Shao C., Wang X., Xie X., Zhang X., Zhang Z., Zhao B., Zhou G., Zhou J. (2013). Carbon fluxes, evapotranspiration, and water use efficiency of terrestrial ecosystems in China. Agricultural and Forest Meteorology 182–183: 76–90. http://dx.doi.org/10.1016/j.agrformet.2013.08.007

Xia J., Niu S., Ciais P., Janssens I.A., Chen J., Ammann C., Afrain A., Blanken P.D., Cescatti A., Bonal D., Buchmann N., Curtis P.S., Chen S., Dong J., Flanagan L.B., Frankenberg C., Georgiadis T., Gough C.M., Hui D., Kiely G., Li J., Lund M., Magliulo V., Marcolla B., Merbold L., Montagnani L., Moors E.J., Olesen J.E., Piao S., Raschi A., Roupsard O., Suyker A.E., Urbaniak M., Vaccari F.P., Varlagin A., Vesala T.,

Wilkinson M., Weng E., Wohlfahrt G., Yan L., Luo Y. (2015). Joint control of terrestrial gross primary productivity by plant phenology and physiology. Proceedings of the National Academy of Sciences 112, 2788–2793. http://dx.doi.org/10.1073/pnas.1413090112

Xie J., Li Y., Zhai C., Li C., Lan Z. (2009). $CO_2$ absorption by alkaline soils and its implication to the global carbon cycle. Environmental Geology 56: 953–961. http://dx.doi.org/10.1007/s00254-008-1197-0

Xu L., Baldocchi D.D. (2004). Seasonal variation in carbon dioxide exchange over a Mediterranean annual grassland in California. Agricultural and Forest Meteorology 1232: 79–96. http://dx.doi.org/10.1016/j.agrformet.2003.10.004

Yang F., Zhou G. (2013). Sensitivity of temperate desert steppe carbon exchange to seasonal droughts and precipitation variations in Inner Mongolia, China. PLoS ONE 8: e55418. http://dx.doi.org/10.1371/journal.pone.0055418

Yang F., Zhou G., Hunt J.E., Zhang F. (2011). Biophysical regulation of net ecosystem carbon dioxide exchange over a temperate desert steppe in Inner Mongolia, China. Agricultural and Forest Meteorology 142: 318–328. http://dx.doi.org/10.1016/j.agee.2011.05.032

Yang X., Zhang K., Jia B., Ci L. (2005). Desertification assessment in China: An overview. Journal of Arid Environments 63: 517–531. http://dx.doi.org/10.1016/j.jaridenv.2005.03.032

Zha T., Kellomäki S., Wang K., Rouvinen I. (2004). Carbon sequestration and ecosystem respiration for 4 years in a Scots Pine forest. Global Change Biology 10: 1492–1503. http://dx.doi.org/10.1111/j.1365-2486.2004.00835.x

Zhang R., Ouyang Z.T., Xie X., Guo H., Tan D.Y., Xiao X.M., Qi J.G., Zhao B. (2016). Impact of climate change on vegetation growth in arid northwest of China from 1982 to 2011. Remote Sensing 8: 364. http://dx.doi.org/10.3390/rs8050364

Zhang W.L., Chen S.P., Chen J., Wei L., Han X.G., Lin G.H. (2007). Biophysical regulations of carbon fluxes of a steppe and a cultivated cropland in semiarid Inner Mongolia. Agricultural and Forest Meteorology 146: 216–229. http://dx.doi.org/10.1016/j.agrformet.2007.06.002

Zhou J., Zhang Z., Sun G., Fang X., Zha T., McNulty S., Chen J., Jin Y., Noormets A. (2013). Response of ecosystem carbon fluxes to drought events in a poplar plantation in Northern China. Forest Ecology and Management 300: 33–42. http://dx.doi.org/10.1016/j.foreco.2013.01.007